APPENDIX F

ACOUSTIC PROPERTY EXPERIMENTAL RESULTS

F.1 Attenuation of Common Bridge Steels

F.1.1 Introduction

Unexpected observations were made during preliminary experimental testing. After similar surface preparation was performed on various steel specimens, more than 4 dB difference in amplitude was found between SDHs located at a depth of 0.5" in 6 different steel specimens when using a 5 MHz shear wave probe. Currently the AWS D1.5 procedures (for conventional UT and Annex K) explicitly assume that all carbon bridge steels possess the same attenuation characteristics and no correction or consideration needed to be taken during the inspection of bridge welds. As a result, the difference in attenuation found during this preliminary testing directly led to a controlled experimental evaluation of the ultrasonic attenuation in different base metals typically used in bridge construction. The objective was to investigate the effect of different variables, such as ultrasonic frequency, wave mode, material microstructure, and material acoustic velocity, on the magnitude of material attenuation.

F.1.2 Specimen Properties

Nine steel specimens were fabricated and tested using conventional UT and PAUT. Table F-1 outlines the samples tested and their properties. Two specimens, ID 50 and ID 36, were removed from the least and most attenuating specimens during the preliminary experimental testing. To fully evaluate these differences in a more controlled setting, samples were cut from the girders in the field and brought into the laboratory. ID 36 was a "historical" A36 steel, and ID 50 was a modern A709 Gr. 50 steel. Further an additional seven "modern" high performance steels (i.e., HPS) were added to further extend the evaluation. The addition of these new specimens set out to further evaluate if there were differences in the ultrasonic attenuation characteristics in different plates. Three of the new specimens were of the quenched and tempered (QT) variety at the mill, while four of the new specimens were produced using the thermo-mechanical control process (TMCP).

Table F-1. Steel Specimens

ID	Steel Properties	Steel Production Year	Thickness (in)	Width (in)
36	A36	1973[1]	1.25	1.87
50	A709 Gr50	2013	1.25	1.87
70	HPS 70W QT	2015	1.50	1.87
101	HPS 100W QT	circa 2000s	2.00	1.87
102	HPS 100W QT	circa 2000s	1.50	1.87
TMCP 1	HPS 70W TMCP	2009	1.57	1.87
TMCP 2[2]	HPS 70W TMCP	2014	1.25	1.87
TMCP 3	HPS 70W TMCP	2011	2.00	1.87

[1] Date the bridge was put into service

[2] Two specimens, one in the rolled direction and one in the cross rolled direction, were fabricated with this steel plate

The acoustic velocities of the high performance steel samples were measured using an Electro Magnetic Acoustic Transducer (EMAT). Using a shear wave, acoustic velocity was measured in the rolled and cross rolled direction. The acoustic velocities and anisotropic ratios are listed below in Table F-2. (Anisotropic ratio is the measured difference between the acoustic velocities in the rolled and cross rolled directions.) The quenched and tempered specimens, specimens 70 and 101, have a very low anisotropic ratios. In comparison, it is clear that the thermo-mechanical processed specimens demonstrate high anisotropic ratios. After the observation was made, an additional literature review was performed to establish if other researchers have observed this same behavior in TMCP plates. It was found that previous research in Japan have documented this effect for TMCP plates [1], [2]. The Japanese JIS Z 3060 UT code [3] specifies that the shear wave velocity be measured in the direction which the inspection will occur in the test object and compared to the calibration block. Depending on the ratio of the shear wave velocity in the calibration block and test specimen, either a new calibration block is required with a velocity which matches the test object more closely or restrictions are placed on the incidence angle that may be used in the inspection. All three TMCP specimens used during this study would have exceeded the limits that would have corrective action as acoustically anisotropic using the Japanese criteria.

Table F-2. Shear Wave Acoustic Velocities of Steel Specimens

ID	Acoustic Velocity (in/µsec)		Anisotropic Ratio (%)
	Rolled Direction	Cross Rolled Direction	
70 (QT)	0.1271	0.1272	0.05
101 (QT)	0.1272	0.1274	0.15
TMCP 1	0.1328	0.1266	4.80
TMCP 2	0.1304	0.1241	4.95
TMCP 3	0.1293	0.1255	3.04

The literature review also revealed that as expected, chemical composition, grain size, and microstructure have all been found to affect the acoustic properties and propagation of sound through material. The chemical composition of each specimen was obtained and found to meet the requirements of its respective ASTM steel standard. For each specimen, a metallurgical analysis of the grain size and microstructure was also performed by an outside consultant (Chicago Spectro Service Laboratory). Figure F-1 shows the grain

structure perpendicular to rolling for each specimen at the central region of the plate magnified at 100X with Nital etchant.

Specimen 36 consisted of a Widmanstätten pattern of ferrite and pearlite. Specimen 50 consisted of ferrite and pearlite. Specimen 70 had a general structure of fine acicular ferrite with small spherical carbides, but also visible were bands of ferrite and low-carbon martensite and bainite. Specimen 101 and 102 consisted of quenched and tempered martensite. The TMCP specimens all had a variation in grain structure near the surface in comparison with the central regions. Specimen TMCP 1 had acicular ferrite with elongated pearlite and long bands of pearlite in the central region. On the near surface region, a fine acicular ferrite and short bands of pearlite were seen. Specimen TMCP 2 had elongated ferrite with bands of pearlite and bainite in the central region. On the near surface region, elongated ferrite and short bands of pearlite and bainite existed. Specimen TMCP 3 had a fine acicular ferrite with patches of pearlite in the central region. On the near surface region, a more refined structure of fine acicular ferrite and patches of pearlite were seen. Specimen TMCP 2 was further analyzed parallel to the rolling direction. Parallel to rolling, the central region and near surface regions both consisted of elongated ferrite with bands of pearlite and bainite.

Grain size measurements were made in accordance with ASTM E112-13 Standard Test Methods for Determining Average Grain Size [4]. Per ASTM E112, grain size measurements can be conducted numerous ways, but all methods include counting the number of grains or number of grain boundaries along a specified line within a known area. A table is provided in ASTM E112 to rate the grain size from 00 up to 14.0, 00 having the largest average grain size and 14.0 having the smallest average grain size. Table F-3 presents the grain sizes measured for the group of specimens. It should be noted, for Specimens 101 and 102, the prior austenite grain size is measured and presented in Table F-3. In this case, the "prior" austenite grain size was that of the steel before quenching and tempering occurred.

Table F-3. ASTM Grain Size Classifications

ID[(1)]	Grain Size	ASTM Grains per Unit Area (in^2) at 100X[(2)]
36	ASTM 2-1/2	2.83
50	ASTM 7	64.0
70 (QT)	ASTM 10	512.0
101 (QT)	ASTM 8	128.0
102 (QT)	ASTM 8	128.0
TMCP 1	ASTM 11 (central)/ ASTM 11 (surface)	1024.0
TMCP 2	ASTM 11 (central)/ ASTM 11 (surface)	1024.0
TMCP 2 (parallel to roll)	ASTM 10 (central)/ ASTM 10 (surface)	512.0
TMCP 3	ASTM 8 (central)/ ASTM 12 (surface)	128.0/ 2896.3

[(1)]Perpendicular to rolling direction unless noted otherwise

[(2)]ASTM E112, 2013

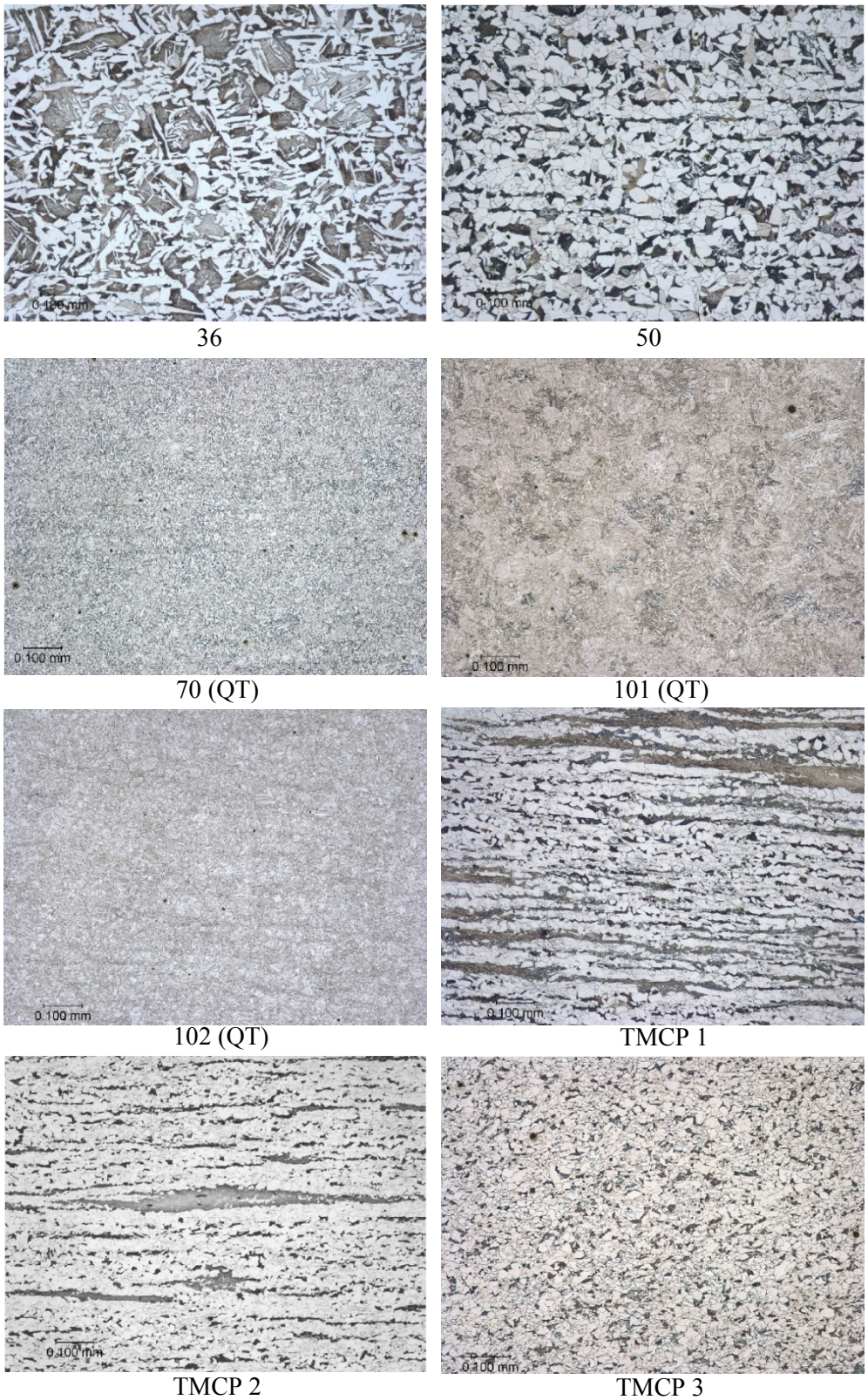

Figure F-1. Microstructure for Specimens at 100X (perpendicular to rolling direction)

F.1.3 Specimen Fabrication and Configuration

The samples were machined into uniform steel blocks. The thickness of the part varied between 1.25" to 2.00" with a consistent width of 1.87" to ensure beam spread did not skew results. The length of the specimen varied based on the available size of steel samples. All specimens were fabricated along the rolling direction with one exception. For TMCP 2, three specimens were fabricated. Specifically, one in the rolled direction, one in the cross rolled direction, and one in the 45° to rolled orientation. The results of the rolled and cross rolled directions are presented in this Appendix while the results in the 45° orientation are presented in Section 3.5.2.2 since testing of this specimen was performed at a later date with different equipment. A CNC machine was used to place four 1/16" diameter SDHs through the full-width of each specimen. Two sets of holes, one at 0.6" and one at 1.0" from the top surface to the center of the hole, were centered in each block at 4" apart. See Figure F-2 for typical fabrication details and Figure F-3 for the final specimens.

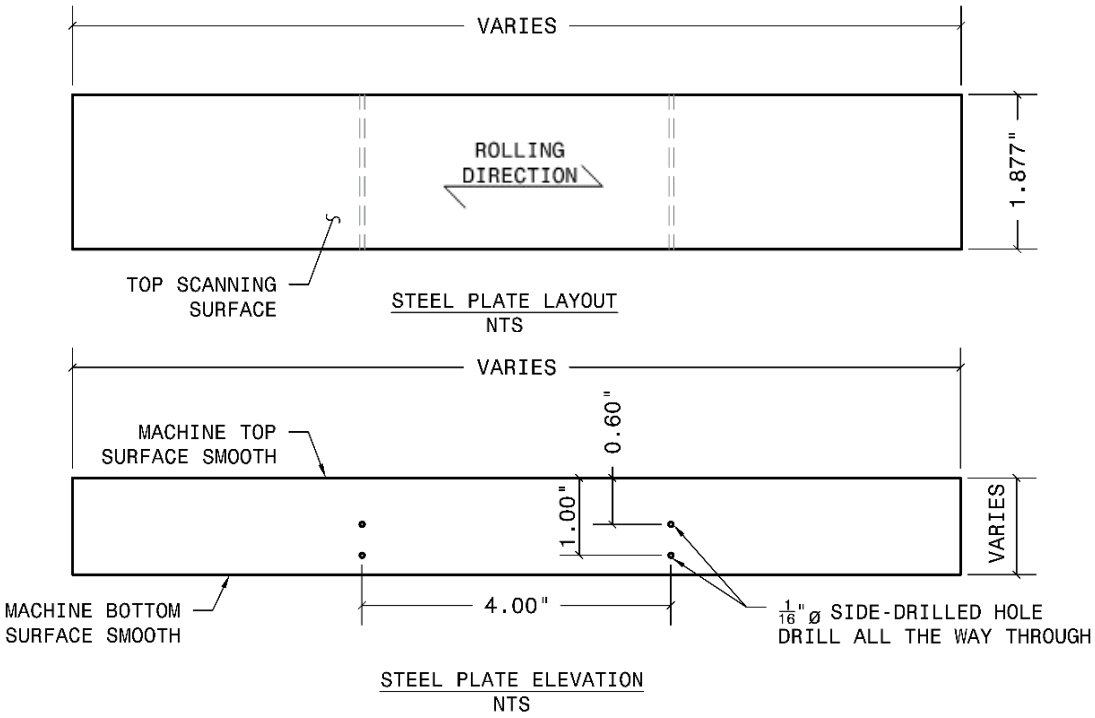

Figure F-2. Typical Fabrication Details for Steel Plate Specimens

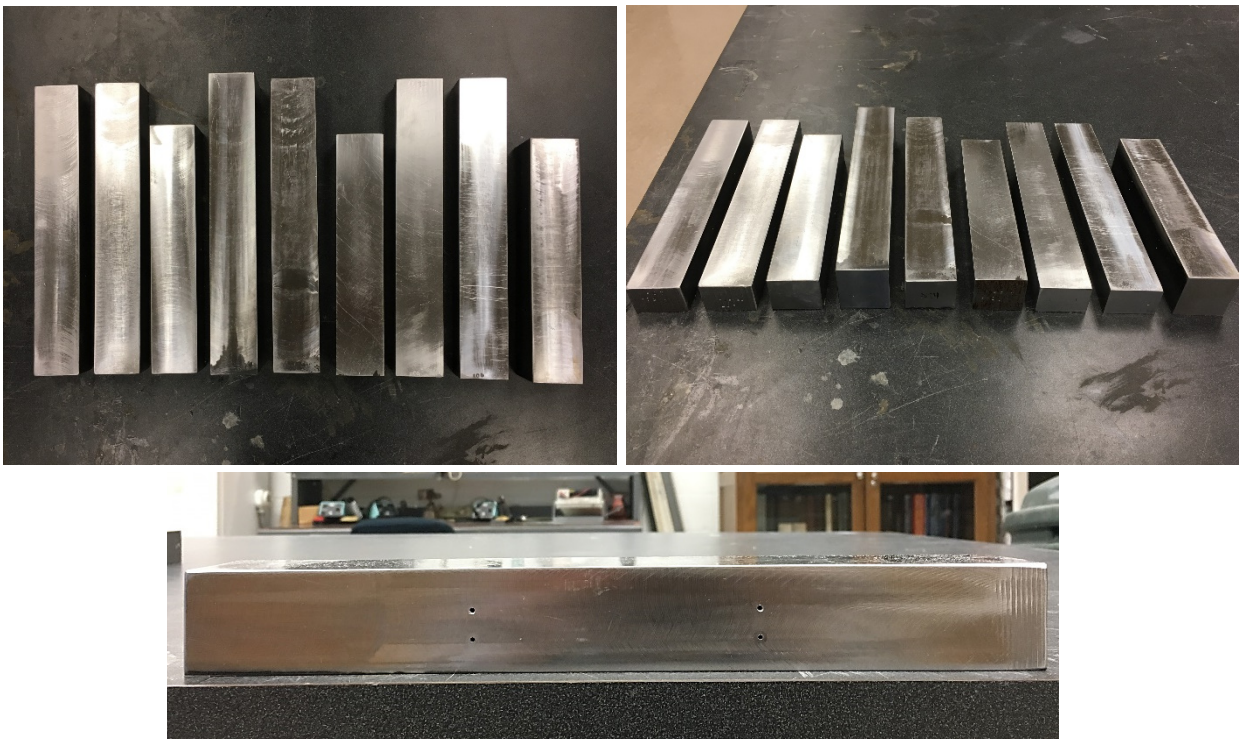

Figure F-3. Steel Plate Specimens (left to right) 36, 50, 70, 101, 102, TMCP 1, TMCP 2 (roll direction), TMCP 2 (transverse to roll direction), TMCP 3

F.1.4 Evaluation Procedures

It is common practice to use a shear wave probe in the inspection of butt welds. Therefore, minimal testing was conducted using compression wave and the ultrasonic inspection primarily focused on using shear waves.

The specimens listed above in Table F-1 were evaluated in a number of different sequences using a combination of different probes and wedges. Table F-4 outlines four test sequences, the number of tests performed within each sequence, the specimens evaluated, the calibration reference, and the equipment used. Sequence 1 evaluated the attenuation of common bridge steels, grades ranging from 36 ksi to 100 ksi, using a 5 MHz PAUT probe, a 2.25 MHz PAUT probe, and a 2.25 conventional UT probe. Sequence 2 evaluated these same specimens using a 5 MHz and 2.25 MHz PAUT probe with compression wave. Due to observed results in sequence 1, sequence 3 was carried out to assess the difference in A36 and 1018 IIW-type reference blocks using the same probes. The evaluation of ultrasonic attenuation of base metal concluded with sequence 4 inspecting thermo-mechanical processed (TMCP) steels using a 5 MHz PAUT probe and a 2.25 MHz conventional UT probe.

The primary reference level was set from the reference block listed in Table F-4. Evaluation then took place for each specimen by peaking the indication signal to 80% full-screen height (FSH). This was done by increasing or decreasing the gain from primary reference level. The increase or decrease in gain revealed whether a specimen was had greater or less attenuation compared with the reference standard, respectively. This evaluation occurred for each hole, in every specimen, and with the probe/wedge combinations outlined below. Shear wave attenuation was investigated at 45°, 60°, and 70° search angles when using conventional UT and PAUT. Each scan of a given SDH was performed a minimum of two times before moving on to ensure the data were repeatable.

Table F-4. Base Metal Tests

Test Sequence-Number	Evaluated Specimens	Reference	Flaw Detector and Probe+Wedge Combination
1-1	0.6" + 1.0" deep holes of Block 36, 50, 70, 101, 102	Block 50 (Side A)	OmniScan MX2 with 5MHz 5L64-A12 + SA12-N55S
1-2	0.6" deep holes of Block 36, 50, 70, 101, 102	Block 50 (Side A)	OmniScan MX2 with 2.25MHz 2.25L64-A2 + SA2-N55S
1-3	0.6" + 1.0" deep holes of Block 36, 50, 70, 101, 102	Block 50 (Side A)	OmniScan MX2 with AWS 2.25MHz 0.63" x 0.63" + 45°, 60°, and 70° SF-AWS
2-1	1.0" deep holes of Block 36, 50,70, 101, 102	Block 50 (Side A)	OmniScan MX2 with 5MHz 5L64-A12
2-2	1.0" deep holes of Block 36, 50, 70, 101, 102	Block 50 (Side A)	OmniScan MX2 with 2.25MHz 2.25L64-A2
3-1	0.6" deep holes of Block 36, 50, 70, 101, 102	IIW A36	OmniScan MX2 with 5MHz 5L64-A12 + SA12-N55S
3-2	0.6" deep holes of Block 36, 50, 70, 101, 102	IIW 1018	OmniScan MX2 with 5MHz 5L64-A12 + SA12-N55S
4-1	0.6" + 1.0" deep holes of Block TMCP 1, TMCP 2, TMCP 3	Block 50 (Side A)	OmniScan MX2 with 5MHz 5L64-A12 + SA12-N55S
4-2	0.6" + 1.0" deep holes of Block TMCP 1, TMCP 2, TMCP 3	Block 50 (Side A)	OmniScan MX2 with AWS 2.25MHz 0.63" x 0.63" + 45°, 60°, and 70° SF-AWS

F.1.5 Experimental Results

The ultrasonic evaluation conducted during this phase evaluated different variables including probe frequency, for both compression and shear wave, code approved reference standards, and grade of steel, including processing. The objective of these tests was to assess the attenuation found in various grades of steel and evaluate the impact it may have on the inspection and detection of flaws.

The results have been presented below as the change in decibels (dB) per inch of sound path, that is the difference in dB between the peak signal amplitude of a SDH and the primary reference level divided by the sound path of the compression or shear wave, see Equation 1. Again, Table F-4 outlines which block the primary reference level was set off of for each test sequence. The change in dB per inch thickness is shown along the y-axis and the base metal evaluated during a given test sequence is along the x-axis. Again, positive values indicate an increase in attenuation from reference (i.e., gain was added) and negative values indicate a decrease in attenuation from reference (i.e., gain was removed).

$$\frac{\Delta dB}{in} = \frac{Indication\ Level\ (dB) - \ Primary\ Reference\ Level\ (dB)}{Beam\ Sound\ Path\ (in)}$$

Equation 1

F.1.5.1 Test Sequence 1 – Probe Frequencies with Shear Wave

During the first test sequence two probe frequencies were compared, 2.25 MHz and 5 MHz. Data collected with two separate 2.25 MHz probes, one conventional UT and one PAUT, and one 5 MHz PAUT probe are presented in Figure F-4, Figure F-5, and Figure F-6, respectively. For all figures, a marker indicates the average change in dB per inch for each specimen. Error bars for each marker displays the variation of indication signals measured between the four holes in each block at the three different incidence angles for each sound path. (Note while the sound paths are different, the data were normalized as dB per inch.).

Figure F-4 and Figure F-5 comparing a 2.25 MHz conventional UT probe with a 2.25 MHz PAUT probe yielded very similar results. Specimens 36, 70, 101, and 102 all attenuated 0.1 dB/in more with the 2.25 MHz conventional UT probe when compared to the 2.25 MHz PAUT probe. This is believed to be a negligible difference. The variation between the two probes was likely credited to the difference in probe aperture and size. Therefore, there is no inherent difference in attenuation due to PAUT versus conventional UT.

Further comparing Figure F-4 and Figure F-5 to Figure F-6, a noticeable difference between the attenuation per inch with a 2.25 MHz and 5 MHz probe was observed. All five specimens only varied at most by an average of 0.3 dB/in with a probe frequency of 2.25 MHz, but with a 5 MHz this increased to 1.3 dB/in. This was a more than 300% increase in the average attenuation between all specimens in terms of dB/in. At 2.25 MHz specimens 36 and 50 behaved almost the same, but at 5 MHz they differ by an average of 0.7 dB/in. The high performance steel specimens (all quench and tempered) attenuated less compared to specimen 50 by 0.3 dB/in with a 2.25 MHz probe to 0.6 dB/in with a 5 MHz probe. Clearly, probe frequency played a critical role in attenuation with shear wave. Higher frequencies resulted in larger differences in attenuation between grades of steel.

While frequency amplified the differences observed between various grades of steel, trends between material properties and attenuation were present regardless. The findings of this evaluation coincide with previous research from Papadakis [5] which established an evident relationship between grain size and grain scattering with attenuation. The high performance steels, which have undergone quench and tempering heat treatment, attenuated less than those that have not. From the analysis of the microstructure, the refined grain size of specimens 70, 101, and 102 promoted the transmission of sound and reduced attenuation.

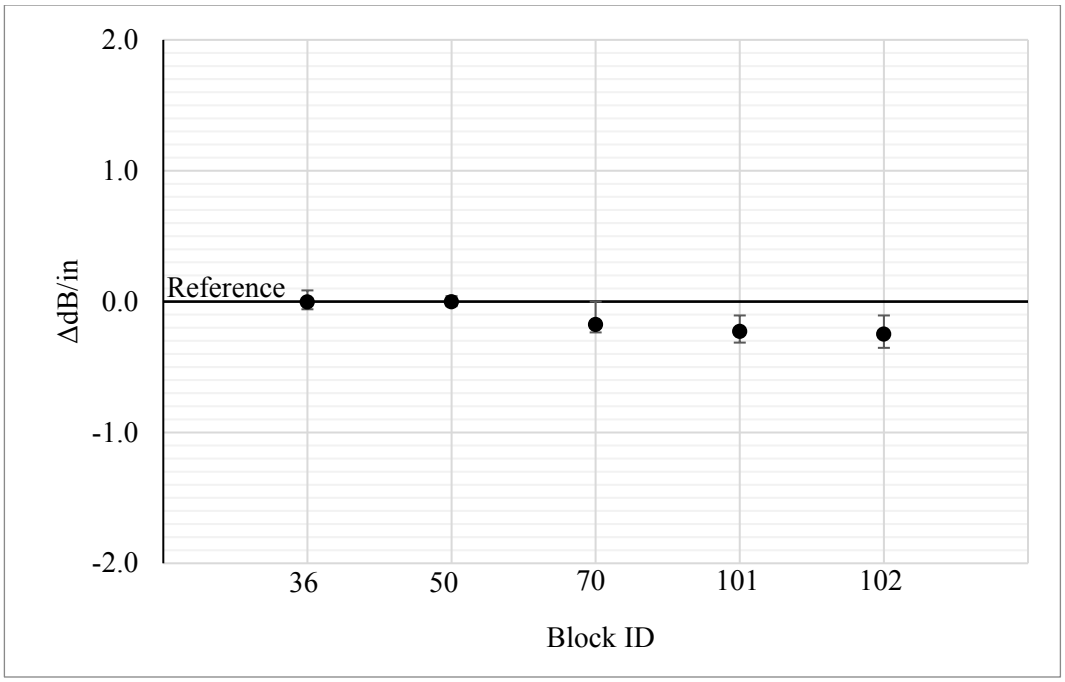

Figure F-4. Change in Attenuation Per Inch of Sound Path – 2.25 MHz Conventional UT

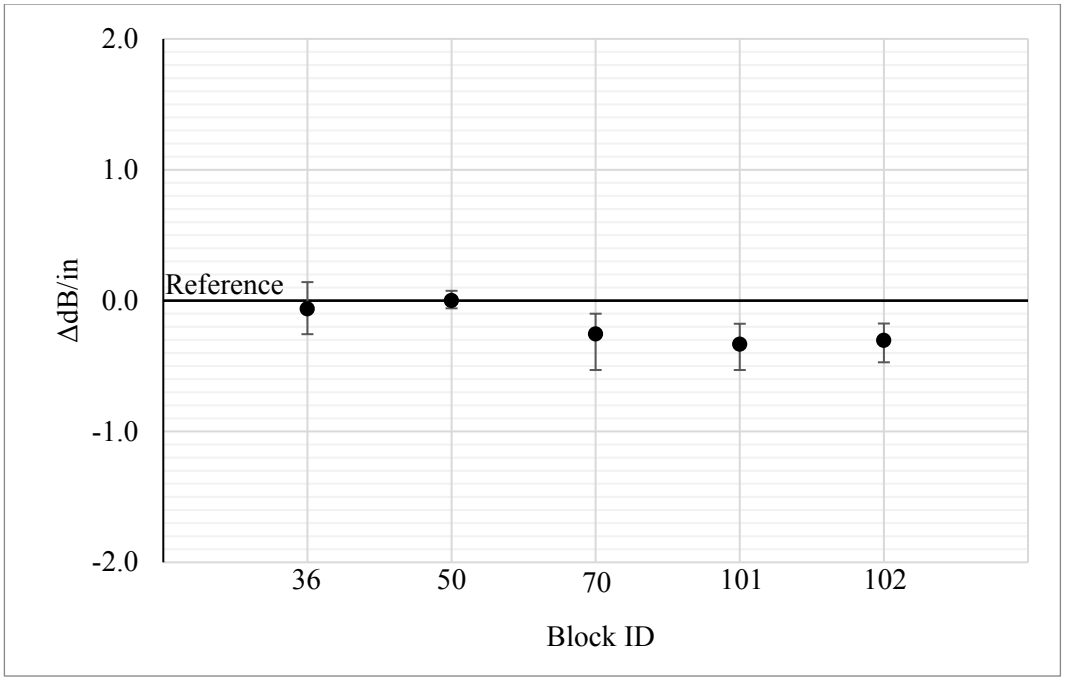

Figure F-5. Change in Attenuation Per Inch of Sound Path– 2.25 MHz PAUT

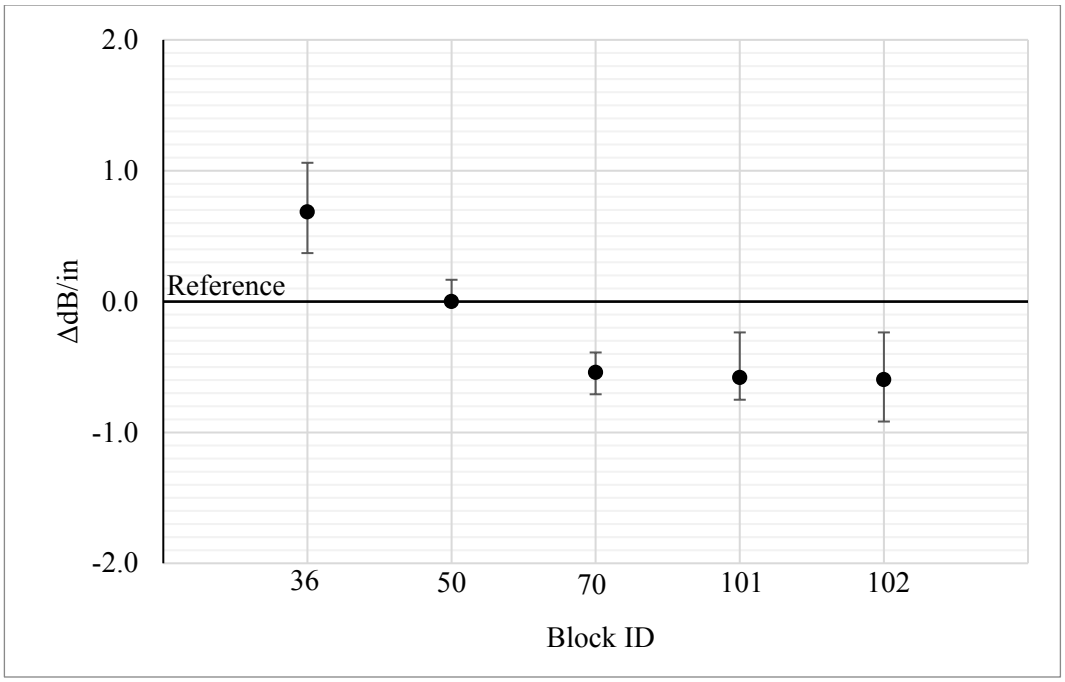

Figure F-6. Change in Attenuation Per Inch of Sound Path – 5 MHz PAUT

F.1.5.2 Test Sequence 2 – Probe Frequencies with Compression Wave

A comparison between compression wave probe frequencies was also investigated. A 2.25 MHz PAUT and 5 MHz PAUT probe were used to inspect five different steel specimens. Similar to above, a marker indicates the average change in dB per inch for each specimen. Error bars for each marker displays the variation of indication signals measured between the two holes in each block. Figure F-7 and Figure F-8 again showed a clear difference in attenuation per inch of sound path between the two different frequencies. All five specimens only vary 0.6 dB/in with a probe frequency of 2.25 MHz and 1.5 dB/in with a 5 MHz probe frequency. This was a more than 150% increase in attenuation between specimens. Thus, the effect of probe frequency on attenuation was seen for both shear wave and compression wave. Again, regardless of frequency the QT high performance bridge steels attenuated less.

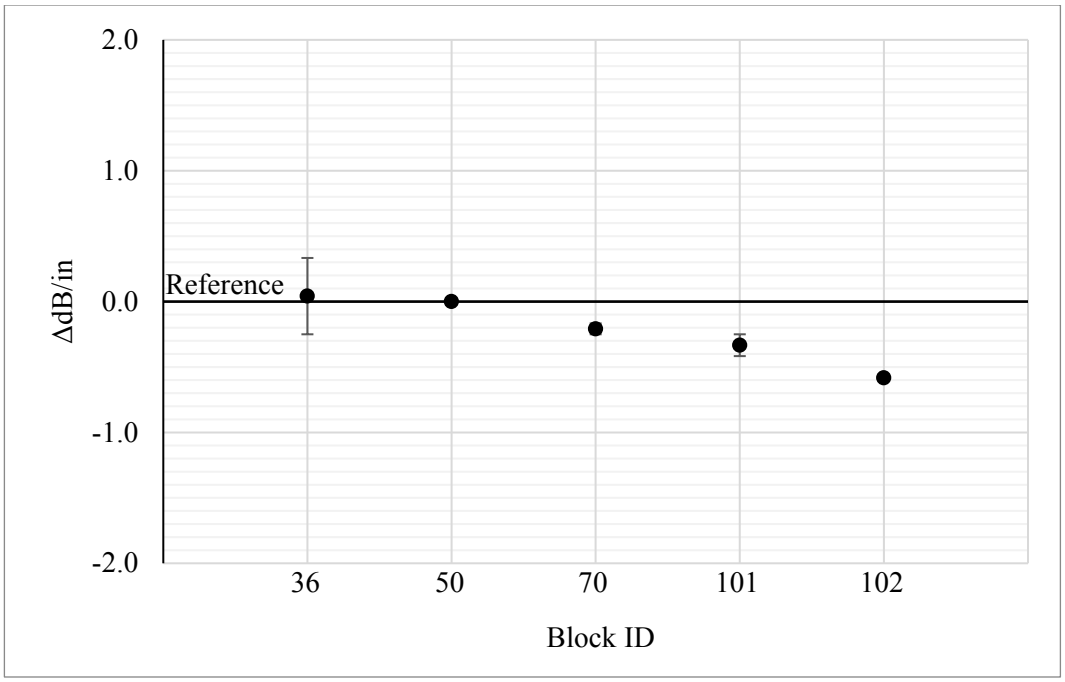

Figure F-7. Change in Attenuation Per Inch of Sound Path– 2.25 MHz PAUT Compression Wave

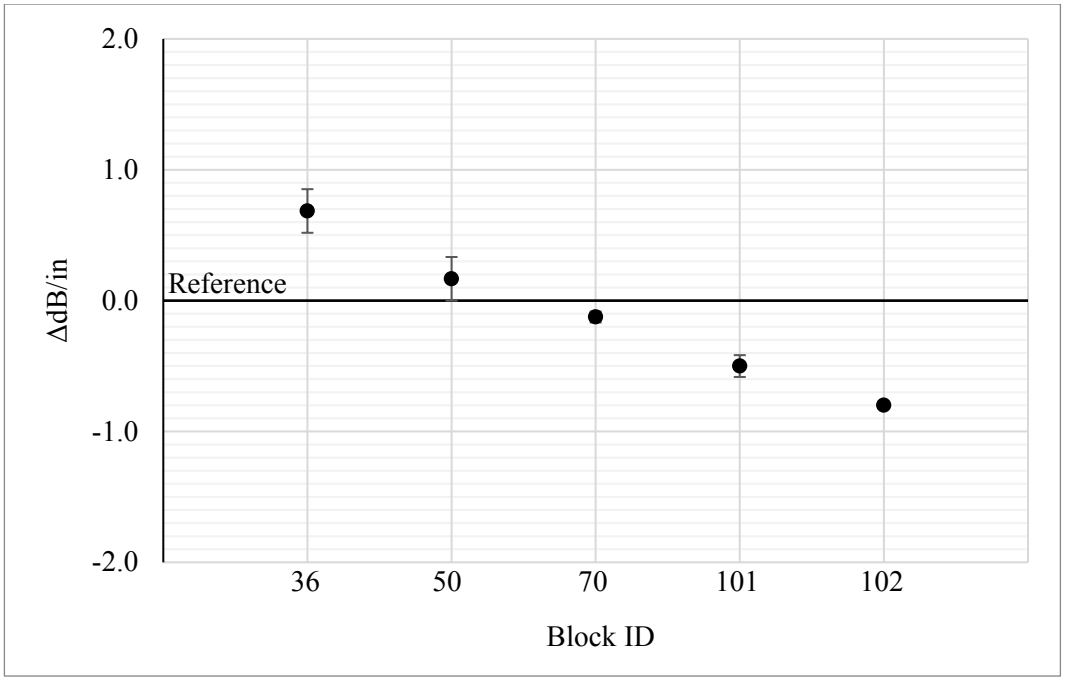

Figure F-8. Change in Attenuation per Inch of Sound Path– 5 MHz PAUT Compression Wave

F.1.5.3 Test Sequence 3 – Difference in Reference Blocks

AWS D1.5 requires an IIW-type reference block to be used as the standard for distance and sensitivity for evaluation using both conventional UT and PAUT. It is important to note that AWS currently refers to this reference block as an 'IIW block' but it is truly an 'IIW-"Type" block. IIW-"Type" reference blocks are formed similar to a "True" IIW block but do not conform to the material requirements of the International Organization for Standardization (ISO) 2400 specification [6]. A true IIW reference block in accordance with ISO 2400 is of steel grade S355J0 and is subject to a very strict heat treatment process. The steel is to be austenitized at 1688 °F for 30 minutes, rapidly quenched in water, tempered at 1184 °F for 3 hours, and air cooled. The measured acoustic velocity of these blocks is required to be 0.233 in/μs ± 0.0012 in/μs for compression wave and 0.128 in/μs ± 0.0006 in/μs for shear wave. An additional margin of error of ±0.2 % is allowed for both the compression and shear wave acoustic velocities.

AWS D1.5 states that the IIW-type reference block should conform to the A709 Gr. 36 specification or acoustically equivalent. Two IIW-type reference blocks conforming to two different material specifications, A36 and AISI 1018, were used to facilitate this phase of testing and would be acceptable reference blocks under the lax guidelines of AWS.

Figure F-9 and Figure F-10 illustrate the results collected using a 5 MHz PAUT probe in shear wave with the two different reference blocks. In comparing the results, it is visible that different results were measured depending on which reference block was used. The A36 calibration block was more attenuating than all specimens, 0.7 dB/in more attenuating than specimen 36 and 2.1 dB/in more attenuating than specimen 102. The 1018 calibration block fell in the middle of the measured specimen attenuations. While the 1018 block was less attenuating than specimens 36 and 50, it was more attenuating than the high performance steels, specimens 70, 101, and 102. The behavior still varied by 0.7 dB/in from specimen 36, but this time only 0.5 dB/in from specimen 102.

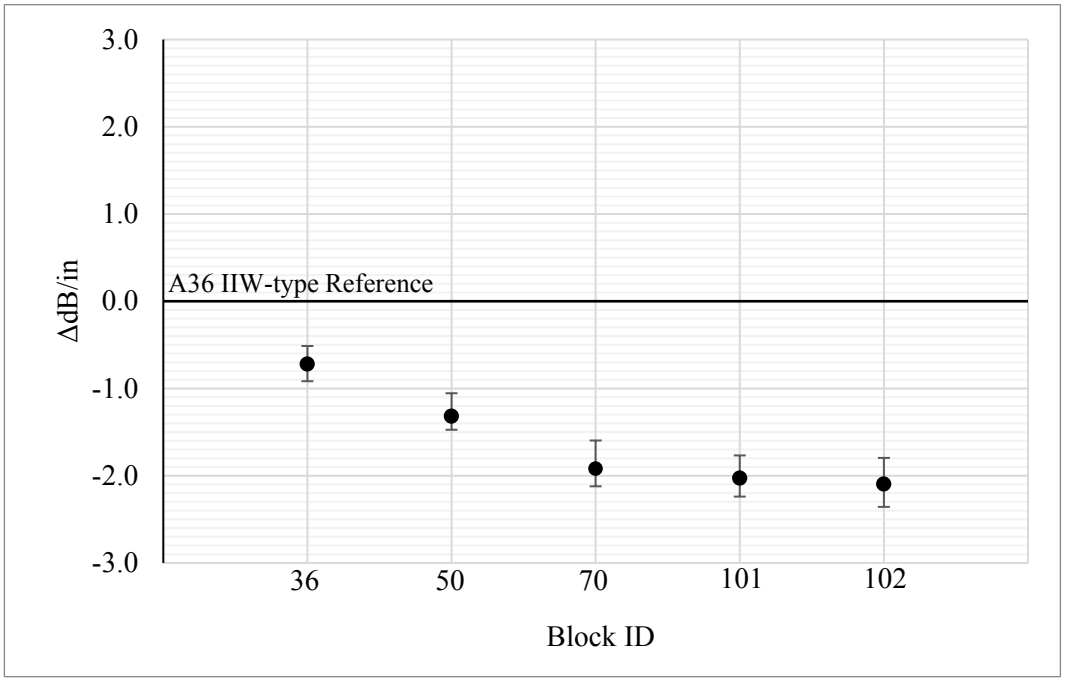

Figure F-9. Change in Attenuation per Inch – A36 IIW-type Reference Block 5 MHz PAUT

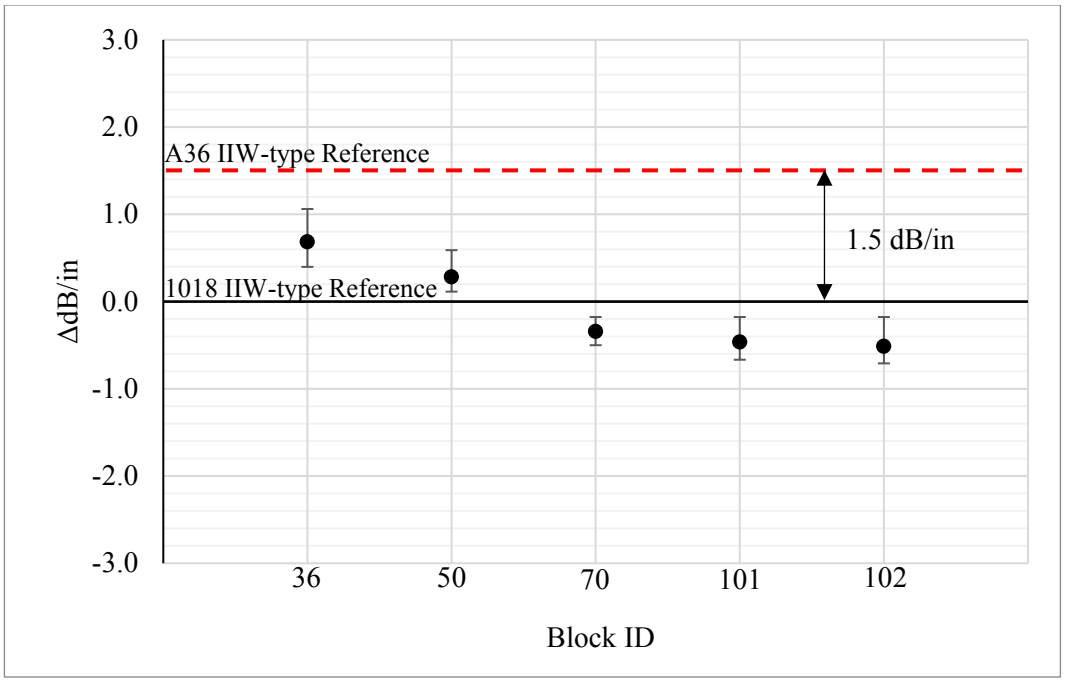

Figure F-10. Change in Attenuation per Inch – 1018 IIW-type Reference 5 MHz PAUT

Concerns arise when the current AWS D1.5 code and its guidelines for IIW-type calibration blocks are considered. Definitive ultrasonic properties are not defined and 'acoustically equivalent' can be very open to interpretation. Even exclusively specifying A709 Gr. 36 could warrant different results if the acoustic attenuation and velocity varies as a result from chemical composition, grain structure, or rolling. Two IIW-type references blocks were tested, one grade A36 and one grade AISI 1018, and the averaged difference in attenuation between the two blocks was of 1.5 dB/in with 5 MHz PAUT. It is unlikely these two specimens account for the extreme maximum and minimum of IIW-type reference blocks currently being used to facilitate ultrasonic inspections, thus this apparent difference could be even larger. Using a 2.25 MHz probe reduced the variation in acoustic attenuation between the A36 and 1018 IIW-type block to 0.3 dB/in.

The IIW-type reference block plays a key role in the acceptance or rejection of flaws during inspection. A difference in material attenuation between different reference blocks, for instance the 1.5 dB/in difference between an A36 and an AISI 1018 IIW-type block, can lead to inconsistency when detecting and characterizing flaws. For example, Figure F-9 shows less gain is required to peak the amplitude signal of a SDH in Block 50 with the A36 IIW-type block while in Figure F-10 gain is added to peak the amplitude signal of the same SDH in Block 50 with the 1018 IIW-type block. In the worst-case scenario, this inconsistency could potentially result in the exact same flaw being automatically acceptable with an IIW-type block but automatically rejectable when a different IIW-type block is used.

Not only does a difference in material attenuation between references blocks themselves matter, but the difference in material attenuation of a reference block and the test object can raise concerns as well. A significant difference in material attenuation between an IIW-type block and a test specimen either results in scanning too sensitive or not sensitive enough. Scanning too sensitive results in a conservative evaluation but will likely result in additional time and cost in repairs of noncritical indications. On the other hand, not scanning sensitive enough causes concerns over the proper rejection of critical flaws.

Evident implications arise when something as simple as the selection of an IIW-type reference block greatly affects the acceptance or rejection results. Currently, calibration is set off a material with different acoustic properties, specifically acoustic attenuation and velocity, than the inspection material. This

difference is not only critical to IIW-type reference blocks but time corrected gain (TCG) calibration blocks, too. AWS D1.5 Annex K requires the use of a TCG calibration block but does not specify nor limit any material properties or geometric constraints for these blocks. In a perfect world, sensitive calibrations and primary reference levels would be set off a material that has the same acoustic properties as the test object (including the weld).

Currently, the International Organization of Standardization (ISO), American Society of Mechanical Engineers (ASME), and Japanese Standards Association require the use of a calibration block with acoustically equivalent (i.e., acoustic attenuation and velocity) properties as the test object [3], [7], [8]. When difference in material attenuation between calibration blocks and test specimens does occur, a transfer correction factor can be implemented. ASME and ISO require a transfer correction to be used to correct for a difference in acoustical properties. ISO specifies a transfer correction is specifically required when a difference of 2 dB to 12 dB at the longest sound path is measured. A transfer correction is formulated by implementing a pitch-catch scanning procedure in a "V" formation and a "W" formation on both materials and measuring the difference in gain between the sound paths.

F.1.6 Conclusions

The evaluation of the ultrasonic attenuation of common bridge base metals yielded the following conclusions:

Test Sequence 1 and 2

- In common bridge base metals ranging from 36 ksi to 100 ksi, an average measured difference in attenuation per inch with shear wave was 0.3 dB/in with a 2.25 MHz frequency probe and 1.3 dB/in with a 5 MHz frequency probe.
- With compression wave, an average measured difference in attenuation per inch in common base metals was 0.6 dB/in with a 2.25 MHz frequency probe and 1.5 dB/in with a 5 MHz frequency probe.
- The change in attenuation between common base metals was more pronounced at higher frequencies. Therefore, the differences in attenuation noticed between 2.25 MHz and 5 MHz frequency probes will result in discrepancies using the current AWS D1.5 Annex K PAUT acceptance criteria.
- Lower frequencies, 2.25 MHz for example, should be used in ultrasonic testing when an amplitude and length acceptance criteria are employed, unless the material attenuation is specifically considered during calibration.

Test Sequence 3

- The ultrasonic properties of calibration materials, such as an IIW-type reference block or TCG block, have a significant impact on the evaluation and classification of bridge components and flaws.
- Two IIW-type reference blocks, one of grade A36 and one of AISI 1018, were used to calibrate and evaluate the base metal specimens. A difference in attenuation of 1.5 dB/in was observed between the two reference blocks using a 5 MHz frequency shear wave probe. This difference was only 0.3 dB/in with 2.25 MHz.
- Due to this difference in attenuation, using the current AWS D1.5 acceptance criteria to evaluate components with sizable differences in ultrasonic properties will lead to a discrepancy in flaw classification. For example, the use of an IIW-type block for TCG calibration that is more attenuating than the test object could lead to flaws being characterized as automatically rejectable, while the use of an IIW-type block that is less attenuating than the test object could lead to the exact same indication as being characterized as automatically acceptable.

- Two solutions to this problem are:
  1) Calibration must occur off a material with the same acoustic properties (acoustic attenuation and velocity) as the test object, unless a transfer correction is performed.
  2) Stringent guidelines for calibration materials and their ultrasonic properties should be outlined in an evaluation code and correspond with the intent of the provided acceptance criteria.

F.2 Shear Wave Velocity

F.2.1 Experimental Results for Test Sequence 4

A separate evaluation of plates from three different heats of high performance steel has been conducted in this section. The steel specimens inspected in this section are all HPS A709 Gr. 70W and have underwent a thermo-mechanical control process (TMCP) treatment. The three specimens have been obtained by three different steel mills in order to look at possible differences in rolling techniques. Again, two different probe frequencies were used to conduct the ultrasonic inspection. Furthermore, one steel sample was used to fabricate specimens in the rolled direction and cross-rolled direction in order to compare the apparent differences in grain structure and ultrasonic velocity.

During the first round of testing noticeable differences between the behavior of a TMCP specimen and a quenched and tempered (QT) specimen, both HPS A709 Gr. 70W, were observed. In the TMCP specimen, at higher incidence angles the location of the SDH was measured to be deeper than the actual known position. Figure F-11 graphically shows a steel block specimen, the four SDHs located within it, and the measured flaw depths for specimens QT and TMCP 1 at a 70° incidence angle. PAUT accurately measured depth of the flaw in the QT specimen while in comparison the TMCP specimen always indicated the SDH was deeper than it actually was. Furthermore, the indication signal became very weak in TMCP specimens. Figure F-12 shows screenshots of the QT and TMCP 1 specimens at an equivalent gain. The amplitude of the QT specimen measured at 80% FSH while the amplitude of the TMCP 1 specimen measured only 20% FSH. Also comparing the two S-scans, note the change in color intensity of the signal amplitude between specimens QT and TMCP 1.

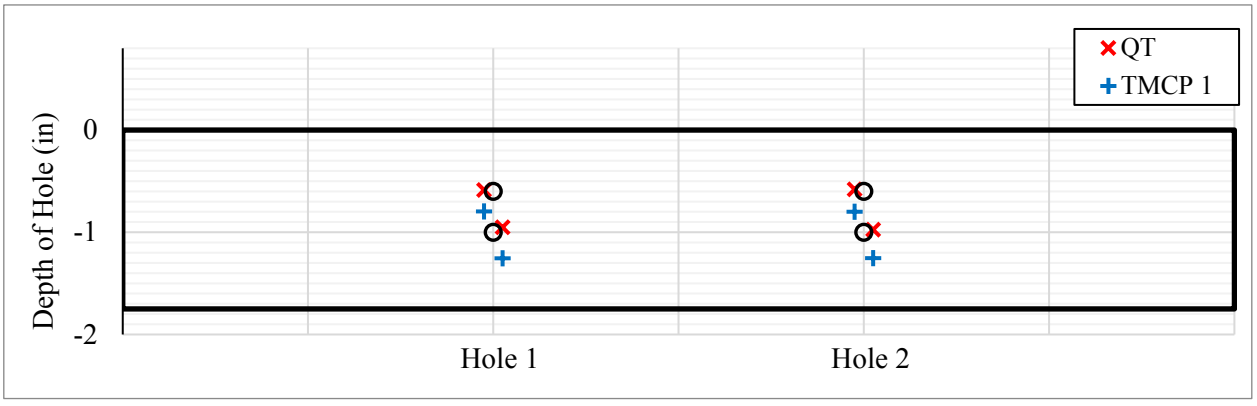

Figure F-11. Recorded Flaw Depth at 70° Incidence Angle

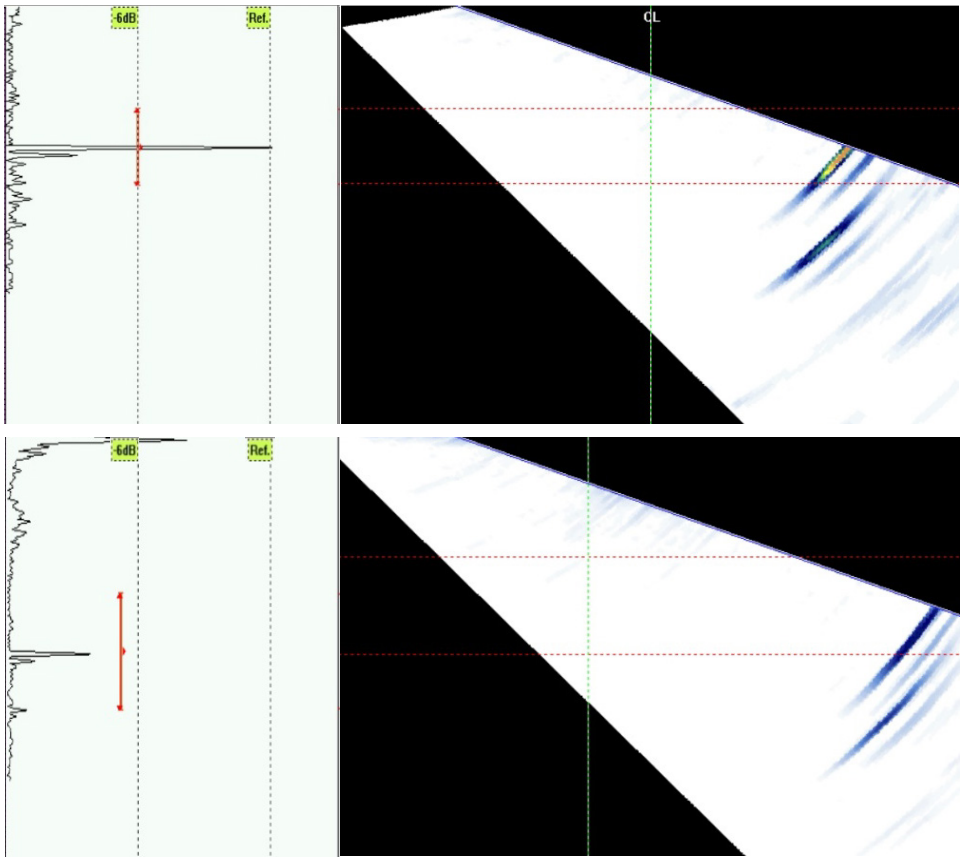

Figure F-12. A-Scan & S-Scan at an Equivalent Gain with 70° Incidence Angle (top) QT Specimen and (bottom) TMCP 1 Specimen

At first, the significant decrease in signal strength was attributed to ultrasonic attenuation in the TMCP specimens. However, after further evaluation and additional research the cause was not a result of attenuation but instead due to the shear wave velocity of the TMCP steel specimens. Accounts of both weakened signals and inaccuracy in locating flaws in steel plates have been reported in previous research studies as a result of acoustic anisotropy, or the variation of acoustic velocity in the rolled and cross-rolled directions. From these studies, the vast majority of plates characterized as acoustically anisotropic were produced using TMCP [1], [2]. The unique behavior observed in these steels has been explained by the increase in the steel's ultrasonic velocity in the rolled direction. This increase in ultrasonic velocity was measured by Rattanasuwannachart et al. to vary through the thickness of a steel plate, being greater at near-surface region versus the central region. The metallurgical reports of specimens TMCP 1, TMCP 2, and TMCP 3 noted the regions adjacent to the surfaces consisted of a different grain structure when compared to the central region. It must be noted that this observation is typical of TMCP plates and does not indicate a problem or abnormality with these specific plates (i.e., the mechanical properties and chemistry meet ASTM A709). Rather, it is simply inherent of the processing associated with TMCP. The near-surface grain structure has been found to cause an increase in ultrasonic velocity. When the shear wave velocity of a given material is significantly faster than the assumed shear wave velocity, the refraction angle of the sound beam is significantly affected which causes much of the sound to follow the surface at the exterior of the plate rather than penetrating into the plate thickness [2]. Therefore, a portion of the total sound expected to transmit into the steel is unknowingly and immediately lost along the surface of the test material causing a significant loss in signal strength of the SDH reflection.

During this experimental investigation, it became apparent that this reflection of sound at the surface is much more critical at higher incidence angles. Rattanasuwannachart et al. has established a relationship between search angle and what is referred to as 'critical shear wave velocity'. The critical shear wave velocity is the velocity that causes refraction along the surface to occur. When a material's shear wave velocity is less than the critical shear wave velocity, the sound beam can form in the material. Conversely, when a material's shear wave velocity is greater, the sound wave will propagate along the surface [2]. This is a result of Snell's Law and beam spread. Due to the increase in velocity along the rolled direction in the TMCP steels, the angle of refraction is always larger than the intended incidence angle. This difference is amplified at larger search angles. The Japanese JIS Z 3060 code uses a variation of Snell's Law to calculate the angle of reflection when the actual velocity and assumed velocity differ:

$$\boldsymbol{\theta_{refraction} = sin^{-1}\left(\frac{V_{actual}}{V_{assumed}} * sin(\theta_{search})\right)}$$

Equation 2

From Equation 2, less impact is seen on the angle of refraction for a smaller incidence angle (i.e. 45°) than a larger incidence angle (i.e. 70°) due to differences in the actual velocity. Also, at lower incidence angles the deviation between the actual material velocity and the assumed velocity can deviate much more before the angle of refraction causes surface reflection of the beam. A 70° sound beam inherently forms and propagates closer to the surface and therefore even a slight increase in the angle of refraction will cause a greater loss in signal due to the increased formation of surface waves.

An evaluation of the three TMCP specimens using 2.25 MHz and 5 MHz shear waves is seen in Figure F-13 and Figure F-14, respectively. Due to the influence of ultrasonic velocity and grain structure on different incidence angles and south paths, the data has been separated by incidence angle and reflector depth along the x-axis. The difference between the indication level and the primary reference level, or the change in dB, per inch thickness is plotted along the y-axis.

Figure F-15 and Figure F-16 show the collected data for the 0.6" deep holes in the three TMCP specimens evaluated with a 2.25 MHz and 5 MHz probe, respectively. Similar to Figure F-13 and Figure F-14, the data has been separated by incidence angle along the x-axis. The difference between the indication level and the primary reference level, or the change in dB, is plotted along the y-axis. Figure F-15 and Figure F-16 directly show the adjustment in gain required to peak signal amplitude of the SDH signals compared to reference. For specimens TMCP 1 and TMCP 2, an average 10.5 dB was added to peak the signal with a 2.25 MHz probe at 70° and an addition of 9.5 dB was required with a 5 MHz probe at 70°. This is a substantial increase compared to specimen 70 (QT) where 1.0 dB was subtracted to peak the signal with a 2.25 MHz probe at 70° and 1.9 dB was subtracted with a 5 MHz probe at 70°.

Trends noted during the ultrasonic evaluation of the three different TMCP specimens are as follows:

- From Figure F-13 and Figure F-14, it is apparent that the three specimens, all of which were from different heats, had differences in their behavior at different incidence angles and sound paths. The differences were small at 45° and 60° but increase significantly at 70°. Figure F-15 and Figure F-16 also show this trend.
- All SDHs, at all angles, and with both frequency probes had lower reported amplitudes than the HPS A709 Gr. 70W QT steel specimen (with the exception of the TMCP 2 0.6" deep SDH at 45° with 2.25 MHz).
- Signal amplitude was most comparable to the HPS A709 Gr. 70W QT specimen at a 45° incidence angle. A weakened signal was observed in all three specimens when compared to the QT specimen at a 60° incidence angle and even more so at 70°.

- The acoustic velocity of specimens TMCP 1 and TMCP 2 in the rolled direction were higher than specimen TMCP 3. As a result, a larger reduction in signal amplitude at 70° was noticed in TMCP 1 and TMCP 2.
- At 60° and 70° incidence angles, the signal amplitude of the 0.6” deep hole was smaller than the 1.0” hole for all specimens. This was unexpected and unusual because the sound path for a 1.0” deep hole is longer than a 0.6” hole. Longer sound paths usually result in an increase reduction of signal amplitude due to material attenuation. However, material attenuation was not the cause of these findings but instead ultrasonic velocity. Thus, this would indicate that the near-surface layer impacted the evaluation of the 0.6” deep SDHs more than the 1.0” deep SDHs. The CIVA modeling showed in APPENDIX E also show the 0.6” hole attenuating more than the 1.0” hole at a 70° incidence angle.
- The use of a 2.25 MHz probe instead of a 5 MHz probe showed no advantage and instead both behaved similarly. Probe frequency was not the cause of the weakened signal amplitudes.

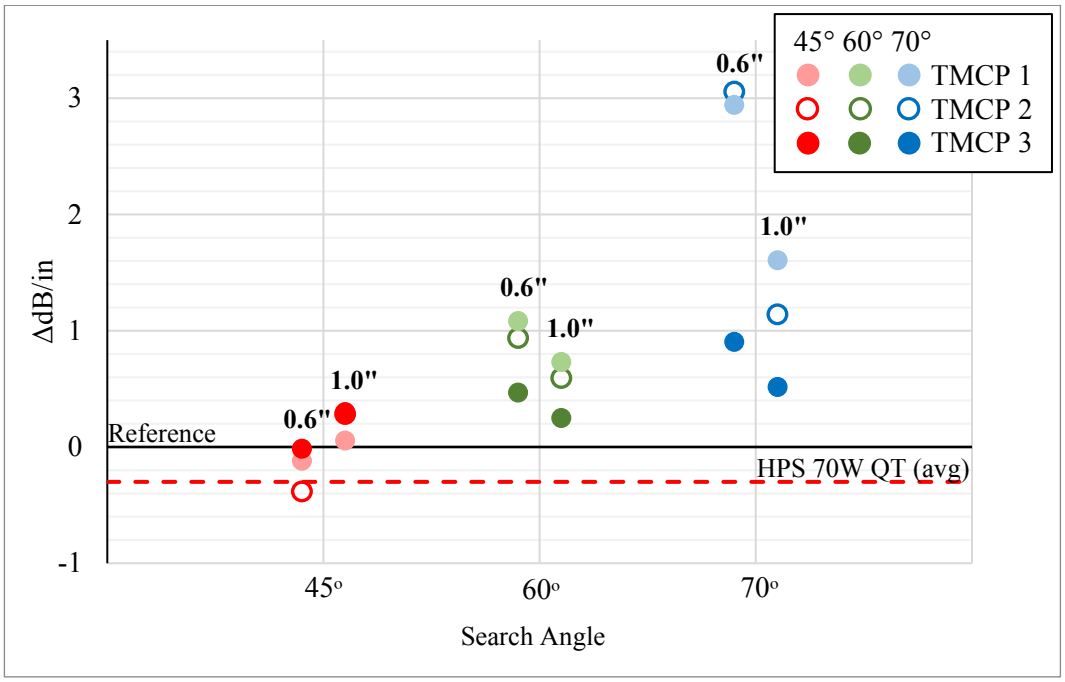

Figure F-13. Change in Signal Intensity per Inch of Sound Path between Incidence Angles – 2.25 MHz Conventional UT

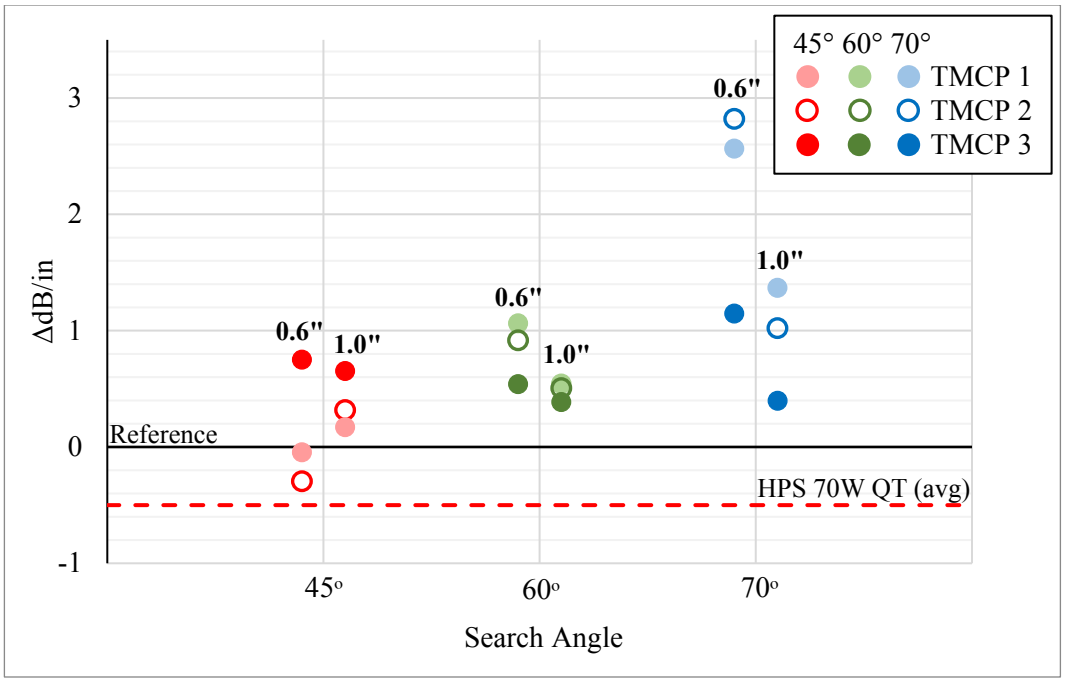

Figure F-14. Change in Signal Intensity per Inch of Sound Path between Incidence Angles – 5 MHz PAUT

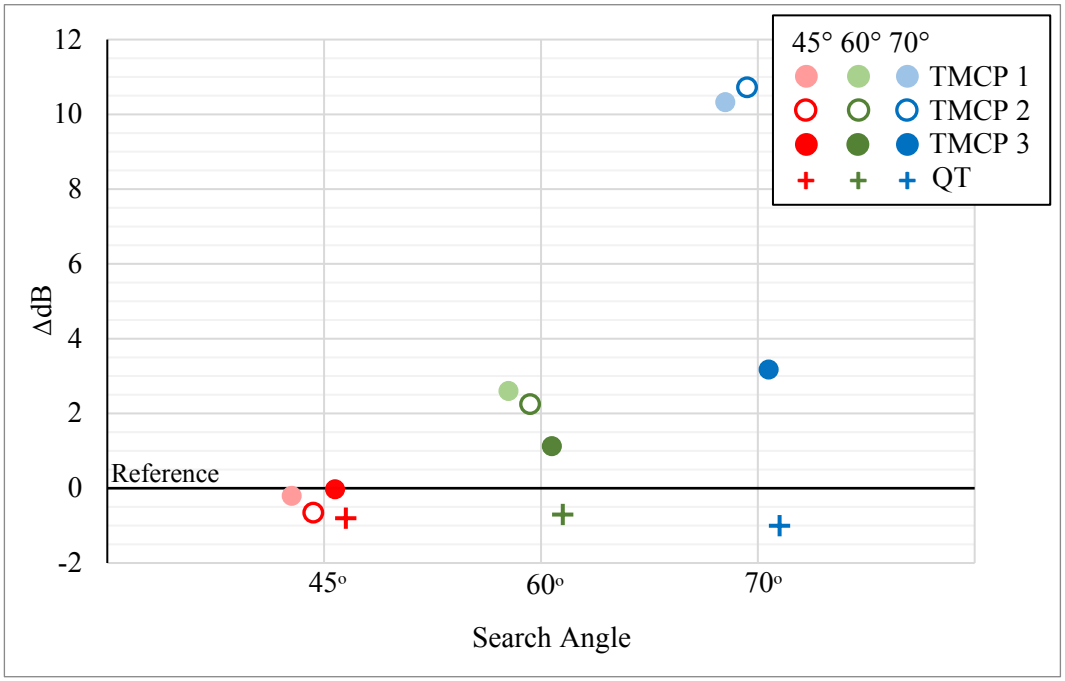

Figure F-15. Change in Signal Intensity between Incidence Angles – 0.6" deep hole, 2.25 MHz Conventional UT

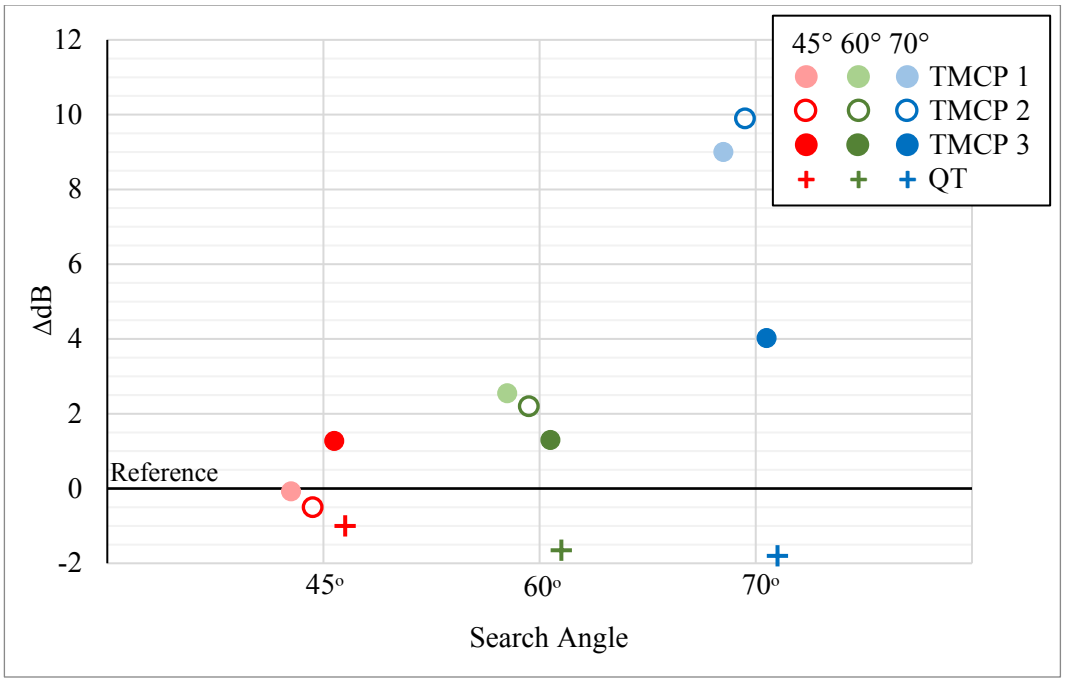

Figure F-16. Change in Signal Intensity between Incidence Angles – 0.6" deep hole, 5 MHz PAUT

The acoustic anisotropy commonly found in TMCP plates is reportedly due to the cooling process and cooling rates during rolling.[2]. To further evaluate these claims, two specimens were initially fabricated from specimen TMCP 2, one in the rolled direction and one in the cross-rolled direction. The data collected in the rolled direction and presented above for TMCP 2 is reiterated below with the addition of data collected in the cross-rolled direction. An additional plate was fabricated at a 45° orientation to the rolling direction from specimen TMCP 2 at a later date to investigate the effect of oblique scanning of acoustic anisotropic plates. The results in the 45° orientation are presented in Section 3.5.2.2 since testing of this specimen was performed at a later date with different equipment.

Figure F-17 and Figure F-18 show the comparison between the rolled and cross-rolled direction of specimen TMCP 2 with a 2.25 MHz and 5 MHz probe, respectively. Again, the data has been separated by incidence angle and reflector depth along the x-axis and change in dB per inch of sound path along the y-axis. From the figures, it was clear the two directions behave very differently. The cross-rolled direction behaved almost identical to specimen 70 (QT) at all incidence angles and with both a 2.25 MHz and 5 MHz frequency probe. The acoustic anisotropy within TMCP steels poses a substantial problem to ultrasonic evaluation, especially if inspectors are unaware of the fabrication practices or material properties of a member being inspected.

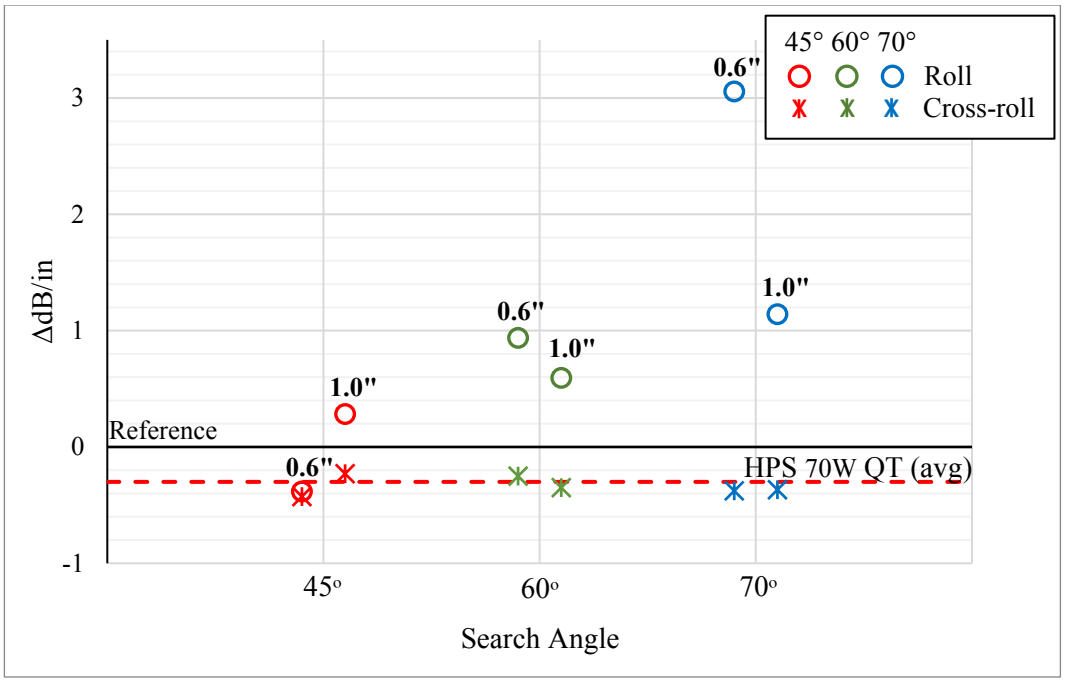

Figure F-17. Specimen TMCP 2 Change in Signal Intensity per Inch of Sound Path – 2.25 MHz Conventional UT

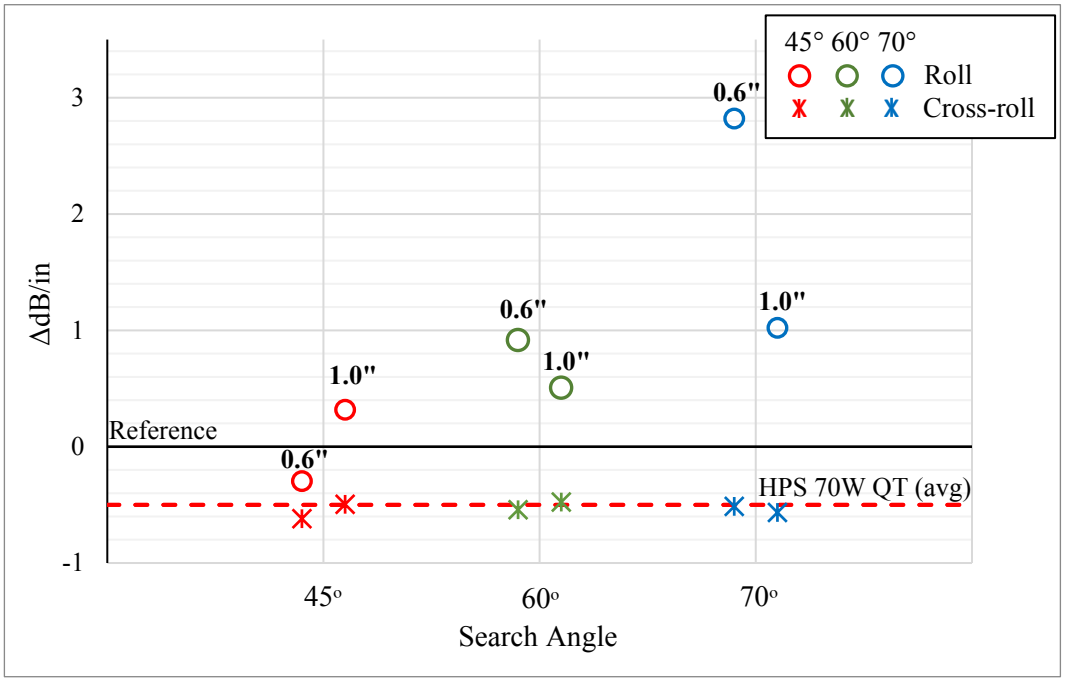

Figure F-18. Specimen TMCP 2 Change in Signal Intensity per Inch of Sound Path – 5 MHz PAUT

F.2.2 Conclusions

The evaluation of the ultrasonic attenuation of common bridge base metals yielded the following conclusions:

Test Sequence 4

- TMCP steel plates are susceptible to ultrasonic anisotropy. Ultrasonic anisotropy affects the detection of flaws at higher incidence angles due to a reduction in signal amplitude. When flaws are detected, accurately locating and sizing the flaws becomes difficult due to a change in the refraction angle.
- Inspection of TMCP plates should be limited to small incidence angles unless the calibration process accounts for the actual shear wave velocity. Previous research suggests limiting the incidence angle to 63° or less [1]. However, experimental testing suggested there is an average 2 dB loss in signal amplitude at 60° than at 45°. Again, the analytical testing with CIVA in APPENDIX E found similar variations in signal amplitude between the different incident angles. Regardless, the increase in signal amplitude at higher incidence angles must be considered during evaluation.
- Probe frequency was not a cause of the large variation in signal amplitude found during the evaluation of TMCP plates. In TMCP plates, the 2.25 MHz probe attenuated very similar to the 5 MHz probe at higher incidence angles.
- The strength of the signal per inch of sound path for the 0.6" deep SDH was consistently lower than the 1.0" deep SDH at higher angles. Therefore, flaws within or closer to the near-surface refined grain structure seen in TMCP plates are affected more by the velocity change.
- Obvious differences in ultrasonic properties between the rolling and cross rolling directions were found in a TMCP specimen. The cross roll direction behaved very similar to a quenched and tempered plate of the same grade, while the rolled direction demonstrated all the characteristics of an anisotropic plate.
- The current AWS D1.5 code does not provide guidance on TMCP or anisotropic plates. The Japanese Industrial Standard's JIS Z 3060 *Method for Ultrasonic Testing for Welds of Ferritic Steel* and the American Petroleum Institute's API RP 2X *Recommended Practices for Ultrasonic and Magnetic Examination of Offshore Structural Fabrication and Guidelines for Qualification of Technicians* both acknowledge and make recommendations with regards to TMCP plates.

F.3 Attenuation of Narrow Gap Improved Electro-slag Welds

F.3.1 Specimen Properties

The variability in ultrasonic inspection of NGI-ESWs was then assessed following the evaluation of base metal. Unlike the consistent microstructure of base metal, welding produces different zones of varying grain structures. From the electroslag welding process, the HAZ consists of two grain structure zones. The portion of the HAZ bordering the base metal is comprised of fine grains and the inner portion is comprised of coarse grains. The weld may have an additional two or three zones itself of coarse columnar and/or equiaxed grains [9]. Specimens were fabricated to facilitate the comparison of attenuation between base metal, HAZs, and weld metal. The electroslag weld samples were donated by the Federal Highway Administration (FHWA) and supplied by two different fabricators. Table F-5 outlines the details of the samples and their material properties.

Table F-5. NGI-ESW Specimen

Specimen ID	Fabricator	Base Metal		Fabrication Year	Thickness (in)
		Side A	Side B		
P1	Fabricator A	HPS 70W (QT)	HPS 70W (QT)	2015	2.0
P2	Fabricator A	50W	50W	2015	2.0
P3	Fabricator A	50W	HPS 70W (QT)	2015	2.0
P4	Fabricator B	HPS 70W	HPS 70W	2013	2.0

F.3.2 Specimen Fabrication and Configuration

Upon receiving the samples, all four were cleaned, polished, and etched to expose the weld and HAZ. The specimens were sanded and etched with 5% Nital. Cross-sections of the weld and HAZs were exposed on both side faces (side 1 and side 2) of the sample as well as the top surface to document how the weld width and shape varies between the two side faces. After exposing the boundaries of the weld and HAZ, proper placement of the reflectors could be determined to achieve the desired sound path. Figure F-19 shows this process for one sample.

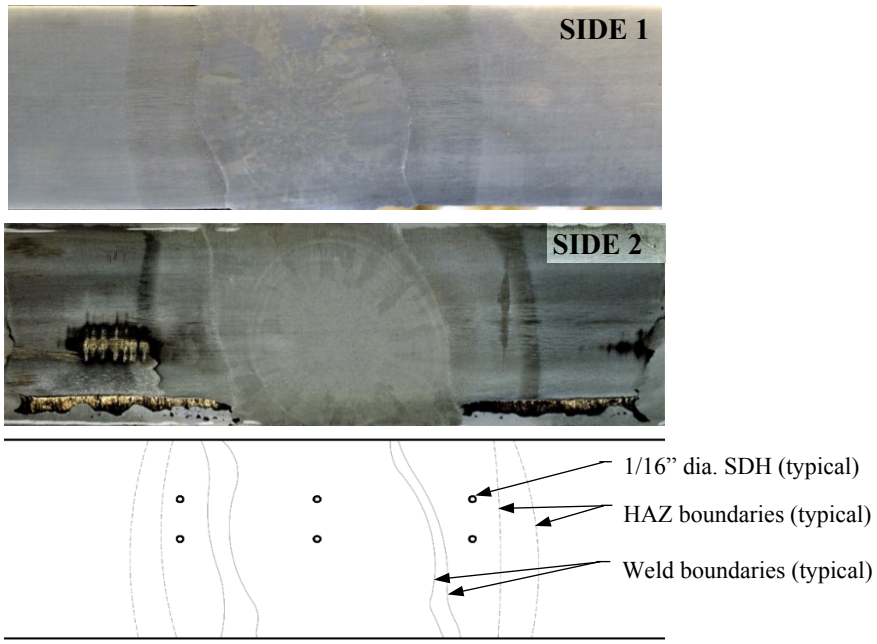

Figure F-19. Specimen P1 Weld and HAZ Boundaries

The four specimens were then individually fabricated using a CNC machine. Eight 1/16” diameter SDHs were placed through the width of the specimen, two in the base metal, two in each HAZ, and two in the weld metal. Holes were placed at 0.6” and 1.0” from the top scanning surface to the center of hole. See Figure F-20 for typical fabrication details and Figure F-21 for the final specimens.

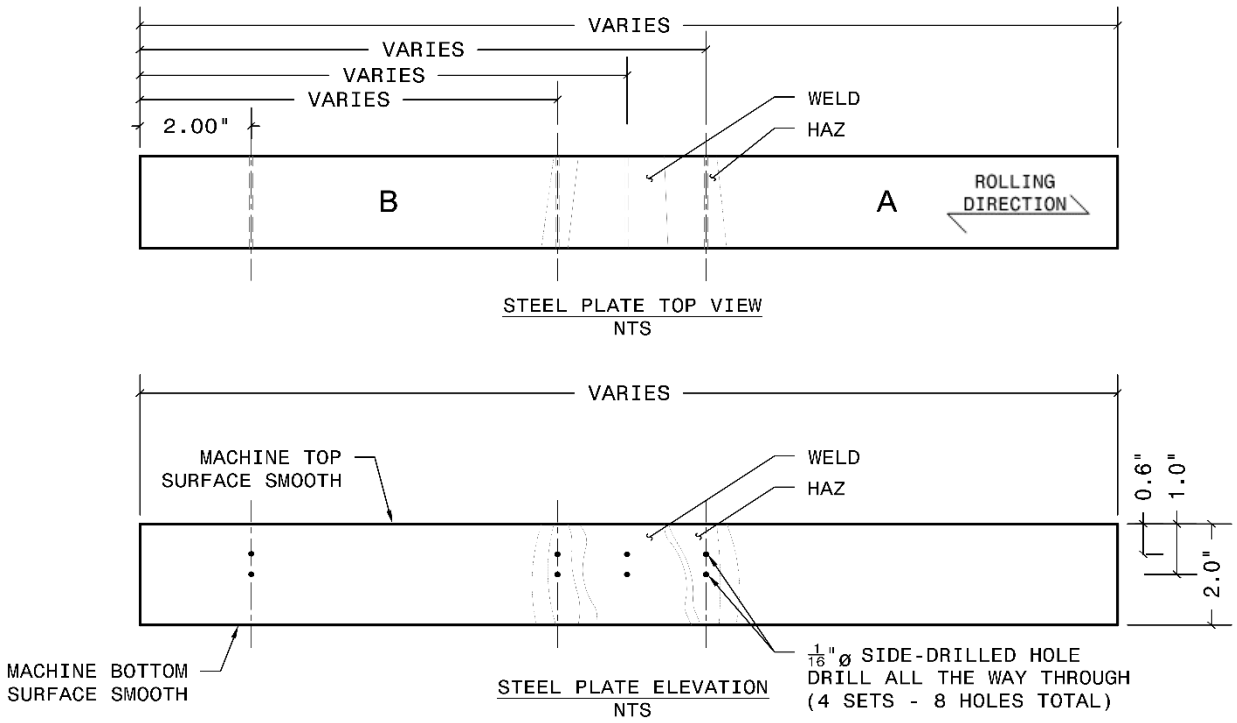

Figure F-20. Typical Fabrication Details for NGI-ESW Specimens

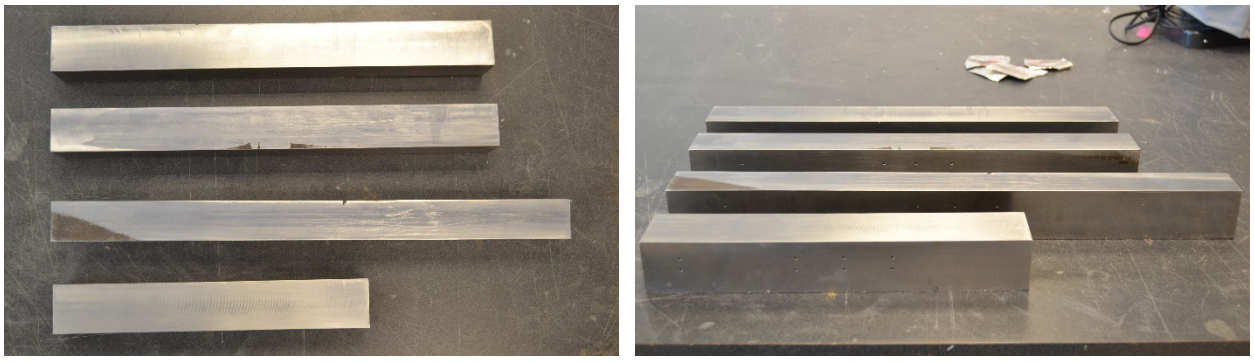

Figure F-21. NGI-ESW Specimens (top to bottom) P1, P2, P3, P4

F.3.3 Evaluation Procedure

The NGI-ESW specimens were assessed with two tests, one evaluating the welds using a 5 MHz PAUT probe and one evaluating the welds using a 2.25 MHz conventional UT probe. Table F-6 outlines the two tests, the specimens evaluated, the calibration reference, and the equipment used. All tests were conducted using shear wave at 45°, 60°, and 70° incidence angles.

The primary reference level was first set from the reference listed in Table F-6. Similar to the base metal procedure above, evaluation took place by peaking the indication signal to 80% FSH. A scan plan was created to ensure the specimens were tested at all incidence angles with sound passing through the base metal, HAZs, and weld metal. A total of 14 data were collected from the 8 SDHs located within each specimen. Evaluation first began by scanning the two SDHs located in the base metal from one side. The SDHs located within the HAZs were then scanned from either side. By scanning the SDHs from either

side, sound initiated in base metal from one side and either in weld metal or the HAZ on the other side depending on the incidence angle. The last holes to be scanned were those located within the weld metal. Again, these holes were scanned from both sides. Due to geometric limitations, scanning took place on the top and bottom surface of the specimens to ensure each SDH was scanned with all incidence angles. Table F-6 provides a typical schematic of the different sound paths of interest.

Table F-6. NGI-ESW Tests

Test Sequence-Number	Evaluated Specimens	Reference	Flaw Detector and Probe+Wedge Combination
1-1	0.6" + 1.0" deep holes of P1, P2, P3, P4	Block 50 (Side A)	OmniScan MX2 with 5MHz 5L64-A12 + SA12-N55S
1-2	0.6" + 1.0" deep holes of P1, P2, P3, P4	Block 50 (Side A)	OmniScan MX2 with AWS 2.25MHz 0.63" x 0.63" + 45°, 60°, and 70° SF-AWS

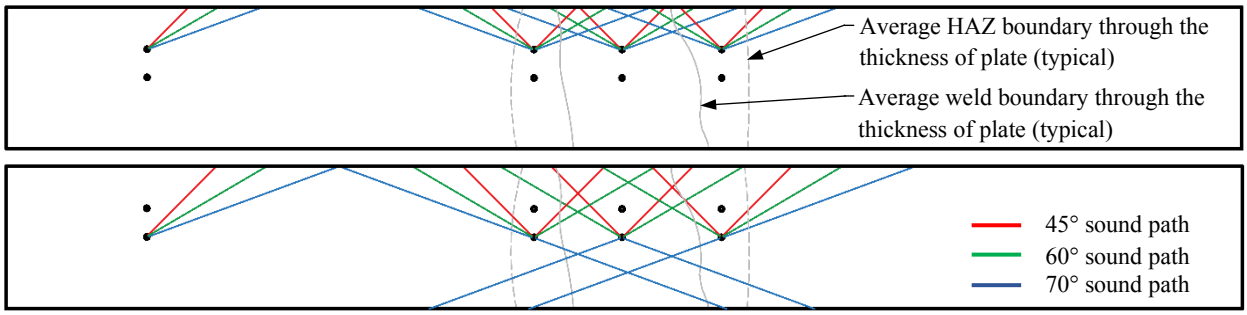

Note: 45° and 60° sound paths from bottom scanning surface not shown for the 1.0" deep SDHs for clarity

Figure F-22. Typical NGI-ESW Sound Path Schematic

F.3.4 Experimental Results

The following sections have been divided by specimens. The figures below all present the data similarly, the hole identification number is along the x-axis along with the different sound paths and change in attenuation per inch of sound path, defined previously by Equation 1, is along the y-axis. The data were grouped this way because the sound path to each hole varied substantially with different incidence angles thus grouping them all together hid the effects of the HAZ and weld metal. For example, at a 45° incidence angle the sound beam would pass entirely through heat-affected base metal, at a 60° incidence angle the sound beam would pass through weld metal and heat-affected base metal, and 70° incidence angle the sound beam would pass through an even larger amount of weld metal and heat-affected base metal. This variation had a considerable impact on attenuation and was noted in the figures below. Two figures show the change in attenuation per inch of sound path of the 0.6" deep holes and two figures show the overall scatter produced when data of the 0.6" and 1.0" deep holes are combined.

Each section shows a schematic of the weld with the average HAZ and weld boundaries and the paths the sound took to each SDH. The sound path to hole 1 was solely though base metal (BM). The sound path to hole 2 was base metal to HAZ from the left and solely HAZ or weld metal (WM) to HAZ from the right. The sound path to hole 3 was solely weld metal or HAZ to weld metal. Finally, the sound path to hole 4 was solely HAZ or weld metal to HAZ from the left and base metal to HAZ from the right. The

figures below designate whether the direction of the sound path came from the right (R) or from the left (L).

F.3.4.1 Specimen P1

Figure F-24 and Figure F-25 show the attenuation per inch of sound path for specimen P1 using a 2.25 MHz and 5 MHz probe, respectively. The overall attenuation of hole 1, hole 2 from the left, and hole 4 from the right were all very similar with both frequency probes. The magnitude of the change in attenuation was larger with a 5 MHz probe than with a 2.25 MHz probe, but from previous experimental results this was expected. The overall attenuation for hole 2 from the right and hole 4 from the left, where the sound path initiated in the HAZ or weld metal, was more inconsistent at different incidence angles and was more attenuating in comparison to when sound initiated in the base metal. The overall attenuation for hole 3 was the most unpredictable and most attenuating.

Figure F-26 and Figure F-27 show the overall scatter in attenuation per inch of sound path for all 8 holes located in specimen P1 using 2.25 MHz and 5 MHz probes, respectively. The intention of these two figures is to illustrate the variation observed between scanning through base metal, the HAZ, and weld metal. Very minimal scatter was seen when both the 0.6" and 1.0" deep holes were inspected at all incidence angles with a sound beam initiating and propagating in solely base metal or base metal (BM) into the HAZ. The average attenuation per inch of sound path was also consistent across three of the holes: holes 1, 2, and 4. The scatter increased when hole 2 and hole 4 were inspected at all incidence angles with a sound beam initiating and propagating in solely the HAZ or weld metal (WM) into the HAZ. With a frequency of 2.25 MHz the overall scatter was an average of 1.7 dB/in for holes 2 and 4. With a frequency of 5 MHz the overall scatter increased to an average of 2.6 dB/in. The largest scatter in attenuation per inch of sound path was observed in hole 3 where the sound beam initiated and propagated solely in weld metal or the HAZ into the weld metal. With a frequency of 2.25 MHz the scatter was 4.4 dB/in and for 5 MHz it was 4.0 dB/in.

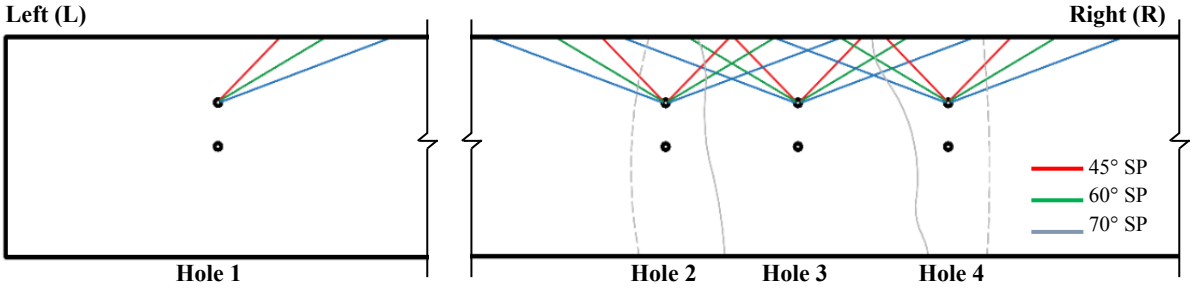

Figure F-23. Specimen P1 Sound Path Schematic – 0.6" deep SDHs

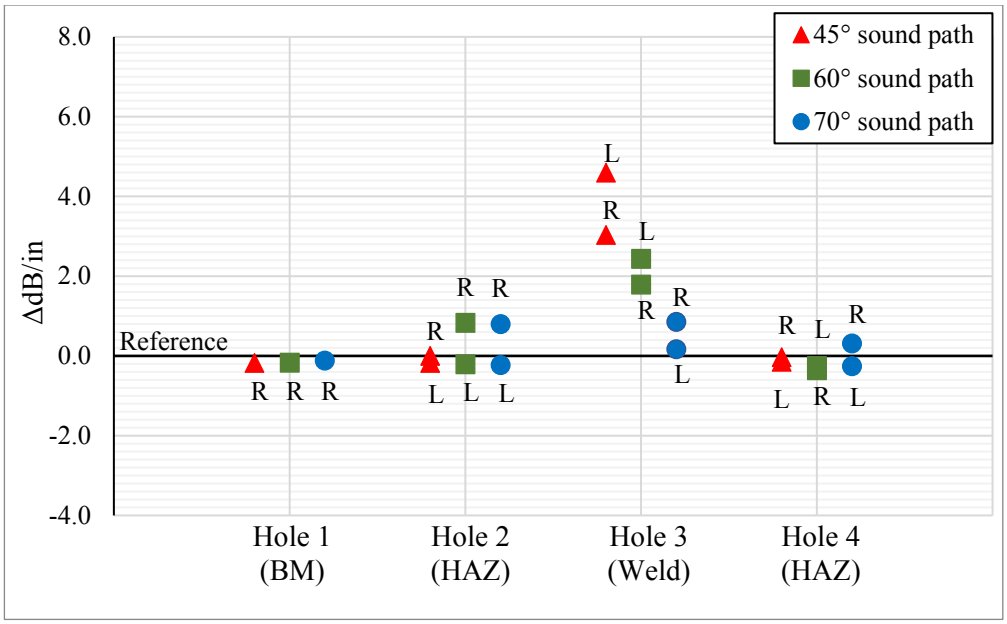

4831
4832 ***Figure F-24. Specimen P1 Attenuation per inch – 0.6 deep hole 2.25 MHz***

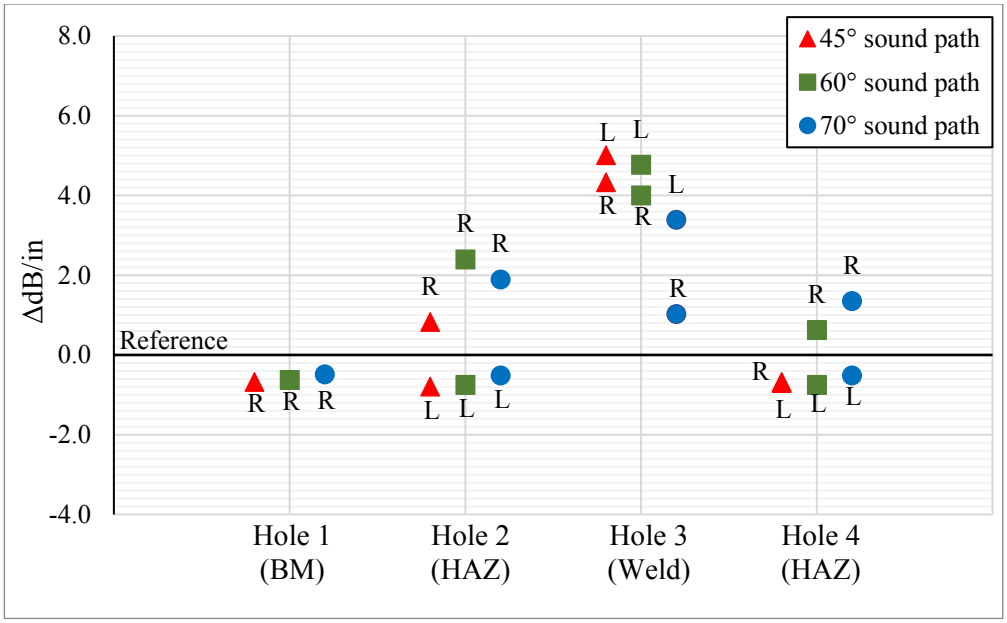

4833
4834 ***Figure F-25. Specimen P1 Attenuation per inch – 0.6 deep hole 5 MHz***

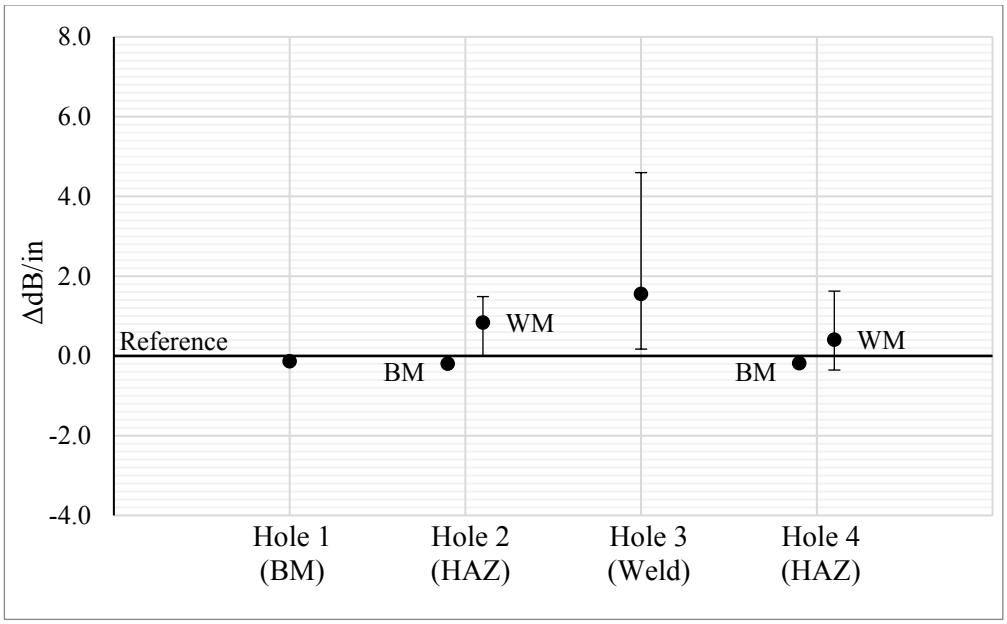

Figure F-26. Specimen P1 Attenuation per Inch Overall Scatter – 2.25 MHz

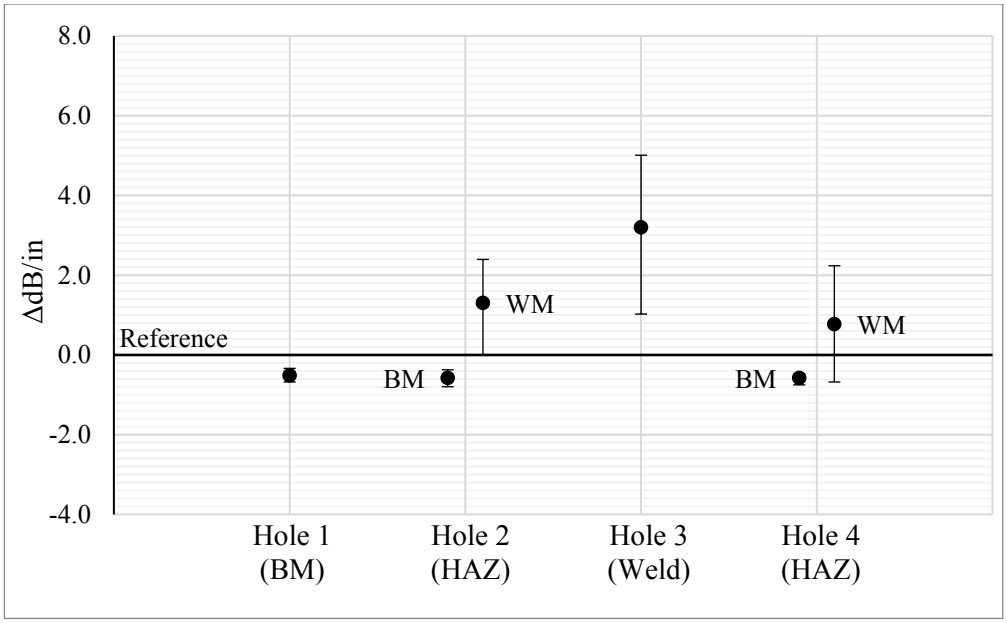

Figure F-27. Specimen P1 Attenuation per Inch Overall Scatter – 5 MHz

F.3.4.2 Specimen P2

Similarly, Figure F-29 and Figure F-30 show the attenuation per inch of sound path for specimen P2 using a 2.25 MHz and 5 MHz probe, respectively. Similar trends in attenuation between base metal, the HAZ, and weld metal were seen between specimens P1 and P2. Overall, the base metal of P2 attenuated more than the base metal of P1 which substantiates the differences in attenuation between A709 Gr. 50 and A709 Gr. HPS-70W QT found earlier. However, with both the 2.25 MHz and 5 MHz frequency probes the average attenuation per inch of sound path in the weld was less in specimen P2 than in P1. Again, the

overall attenuation of hole 1, hole 2 from the left, and hole 4 from the right were the same. In almost all cases, attenuation of hole 2 and hole 4 increased due to the sound initiating and propagating from solely the HAZ or weld metal into the HAZ. Again, attenuation through weld metal for hole 3 varied, but overall the attenuation of the sound traveling through solely weld metal or the HAZ into weld metal was the largest.

Figure F-31 and Figure F-32 show the overall scatter in attenuation per inch of sound path for all 8 holes located in specimen P2 using 2.25 MHz and 5 MHz probes, respectively. Again, the average attenuation per inch of sound path was consistent across holes 1, 2, and 4 where sound was initiated in the base metal. Scatter increased when holes 2 and 4 were shot with sound initiating solely in the HAZ or weld metal. The overall scatter in attenuation per inch of sound path increased to 1.1 dB/in with a frequency of 2.25 MHz and 2.5 dB/in with 5 MHz. In comparison, the overall scatter in attenuation per inch of sound path for hole 3 was 2.6 dB/in with a 2.25 MHz probe and 1.7 dB/in with a 5 MHz frequency.

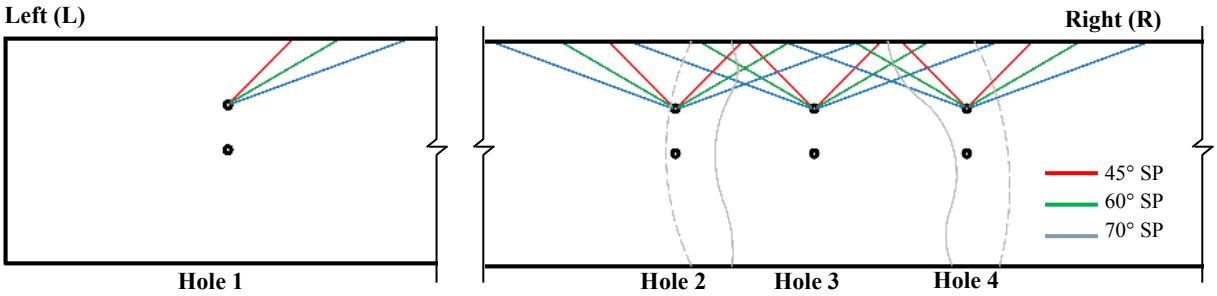

Figure F-28. Specimen P2 Sound Path Schematic – 0.6" deep SDHs

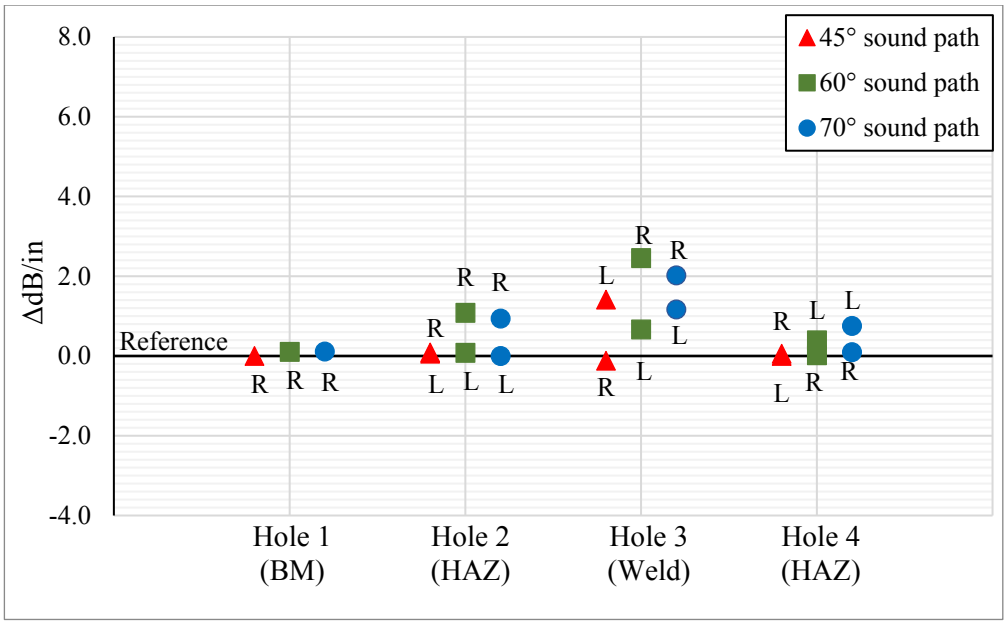

Figure F-29. Specimen P2 Attenuation per inch – 0.6 deep hole 2.25 MHz

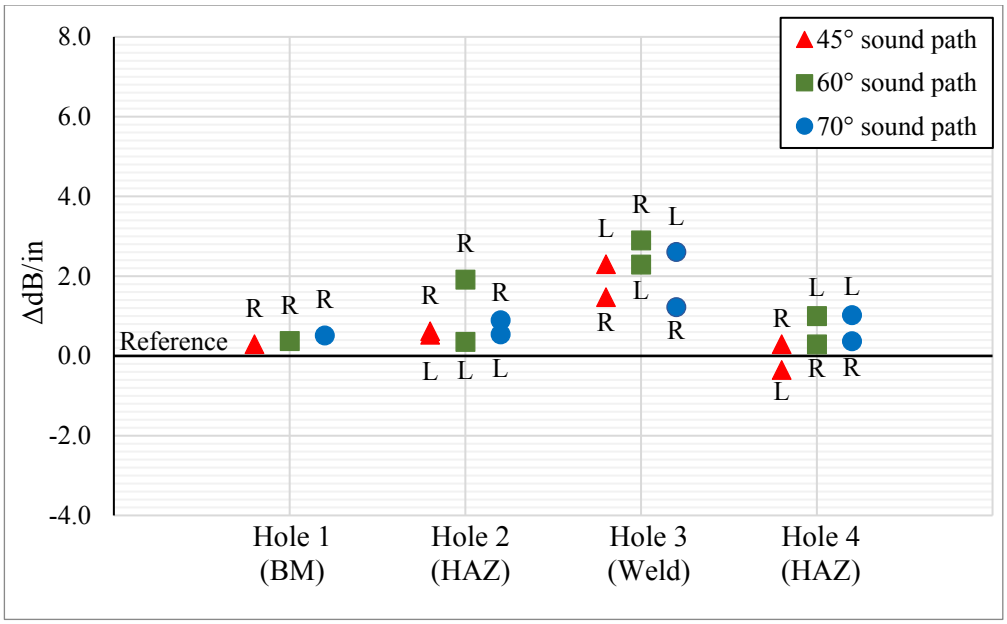

4862
4863 ***Figure F-30. Specimen P2 Attenuation per inch – 0.6 deep hole 5 MHz***

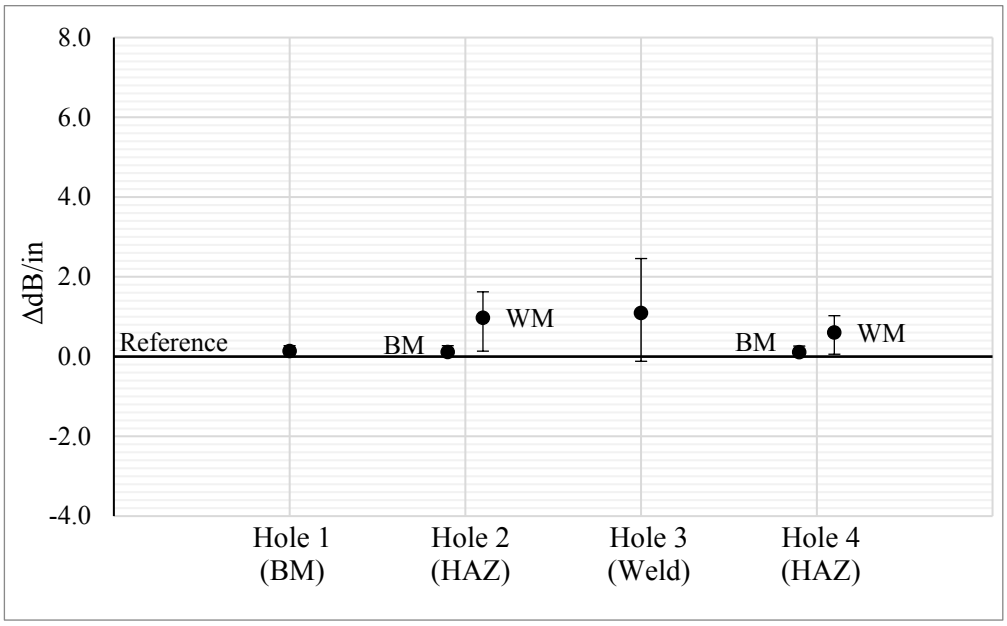

4864
4865 ***Figure F-31. Specimen P2 Attenuation per Inch Overall Scatter – 2.25 MHz***

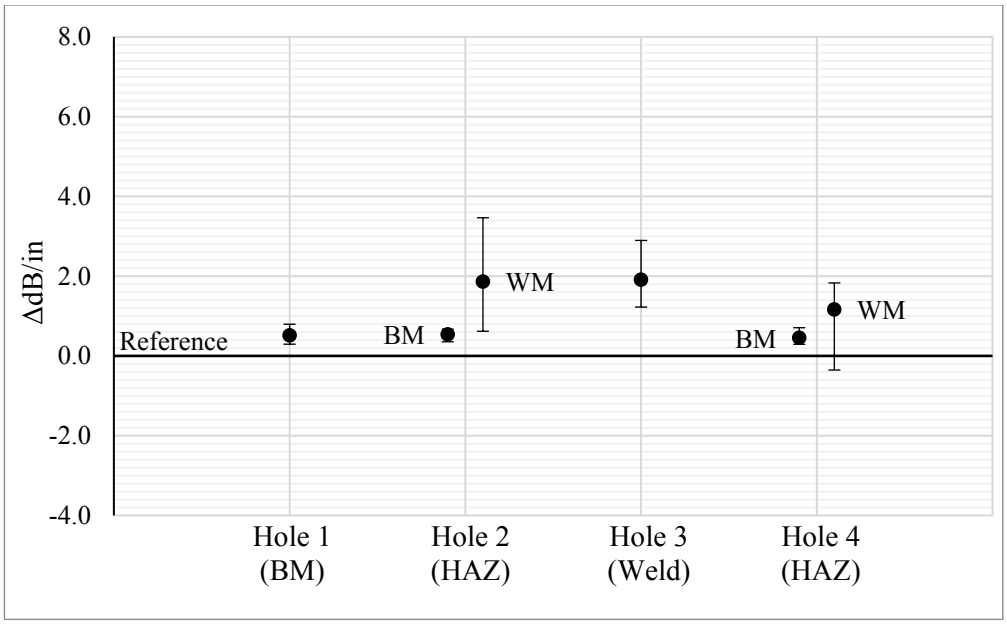

Figure F-32. Specimen P2 Attenuation per Inch Overall Scatter –5 MHz

F.3.4.3 Specimen P3

Specimen P3 was fabricated by the same fabricator as specimens P1 and P2 and was a combination of the two different heats of steels used to fabricate P1 and P2. Therefore, P3 should mimic the results shown above. The left side of P3 was of the same heat of steel as P1 and the right side was of the same heat of steel as P2. Figure F-34 and Figure F-35 show the attenuation per inch of sound path for specimen P3 using a 2.25 MHz and 5 MHz probe, respectively. Attenuation for hole 1 and hole 2, where sound initiated in the base metal, matched perfectly between specimens P1 and P3 for both frequency probes. Attenuation for hole 4 where sound initiated in the base metal matched very similar between specimens P2 and P3 for both frequency probes. Similar variations in attenuation were seen in holes 2 and 4 where sound was initiated in the HAZ or weld metal for specimens P1, P2, and P3.

Figure F-36 and Figure F-37 show the overall scatter in attenuation per inch of sound path for all 8 holes located in specimen P3 using 2.25 MHz and 5 MHz probes, respectively. Again, results for holes 1, 2, and 4 correlated well with the results of specimens P1 and P2. Scatter in attenuation for hole 3 was broken up into side A and side B. The average attenuation per inch of sound path recorded for side A matched specimen P1 within 0.4 dB/in and side B matched specimen P2 within 0.3 dB/in. However, the overall scatter associated with hole 3 in specimens P1, P2, and P3 varied between specimens. Overall, P3 validated the findings and analysis of specimens P1 and P2 above.

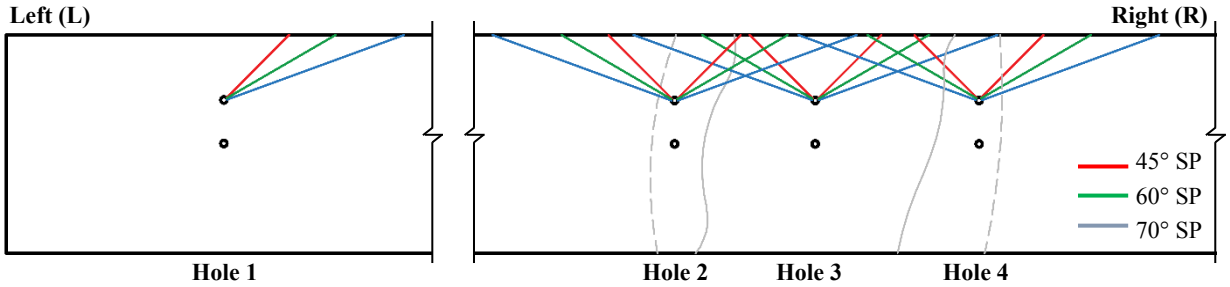

Figure F-33. Specimen P3 Sound Path Schematic – 0.6" deep SDHs

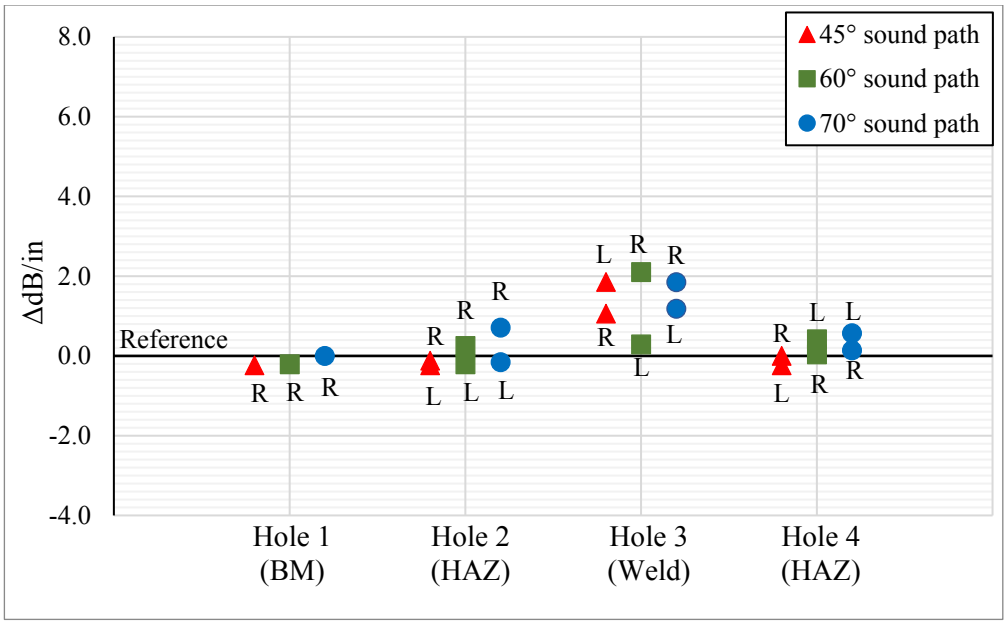

4888
4889 ***Figure F-34. Specimen P3 Attenuation per inch – 0.6 deep hole 2.25 MHz***

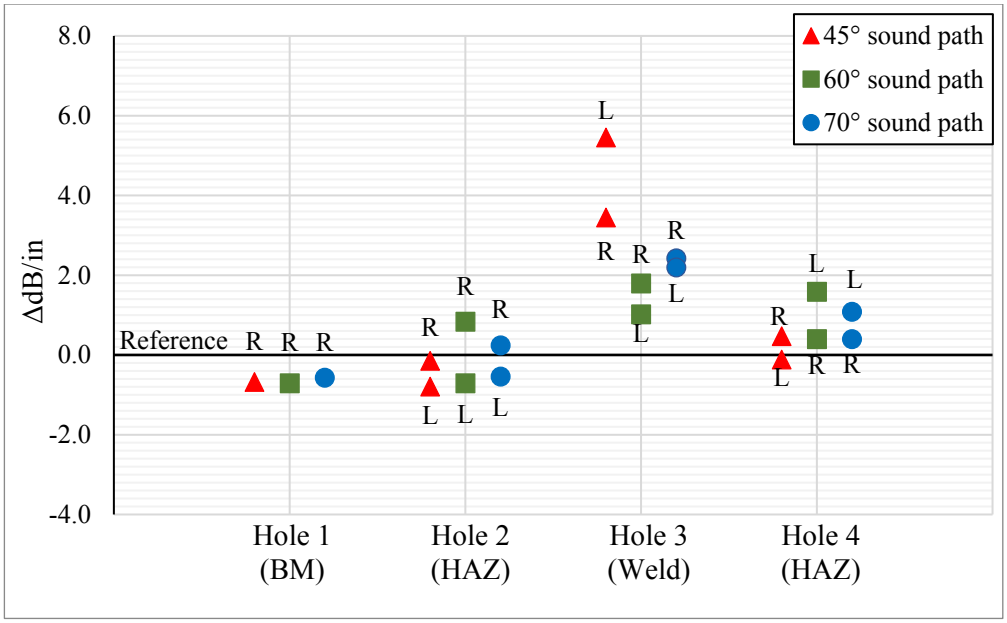

4890
4891 ***Figure F-35. Specimen P3 Attenuation per inch – 0.6 deep hole 5 MHz***

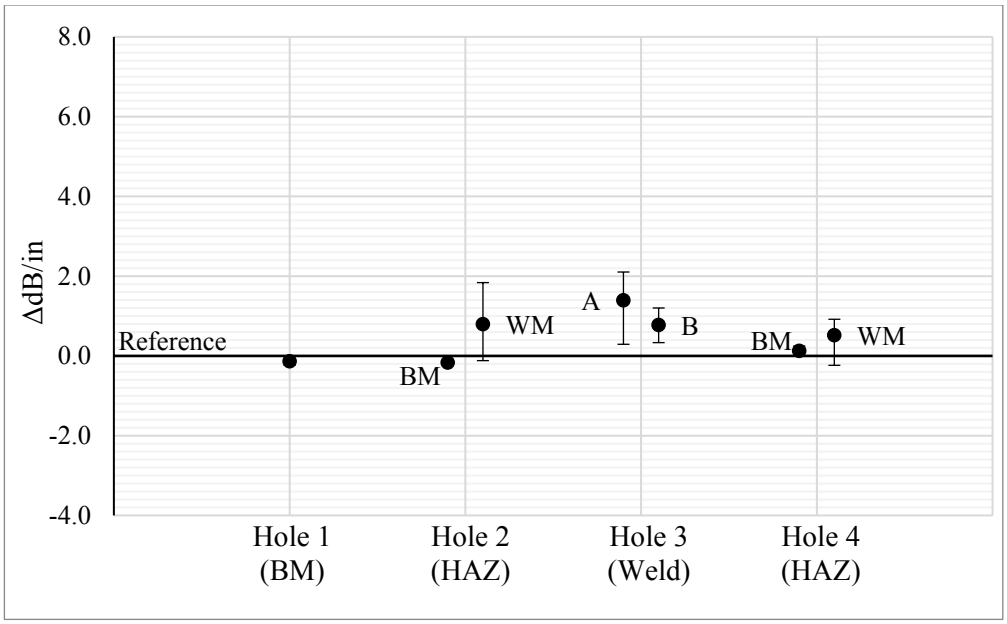

Figure F-36. Specimen P3 Attenuation per Inch Overall Scatter –2.25 MHz

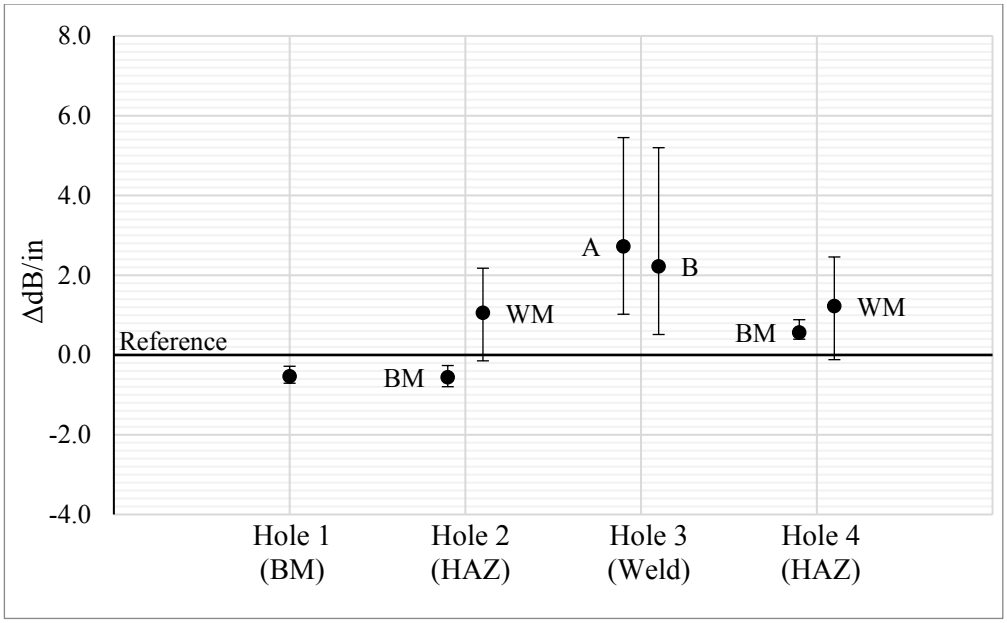

Figure F-37. Specimen P3 Attenuation per Inch Overall Scatter –5 MHz

F.3.4.4 Specimen P4

Specimen P4 was fabricated by a different fabricator than the other three specimens above. While performing the ultrasonic inspection it appeared the base metal of specimen P4 was behaving acoustically anisotropic. A mill report provided for the base metal of this specimen specifically states it was manufactured as QT. The velocity of this plate was measured using a normal incidence angle shear probe and in the rolled direction was found to be 0.133 in/μs and 0.126 in/μs in the cross-rolled direction. It is

the belief of the Research Team that this plate was manufactured using TMCP due to the acoustic anisotropy velocity measurements and the micrographs analyzed by the Research Team.

Figure F-38 compares the results from the 0.6" and 1.0" deep holes in the base metal of specimen P4 to specimen TMCP 1. It was clear the base metal of specimen P4 behaved acoustically anisotropic due to the gradual loss of signal sensitivity at higher angles. While this should not affect the weld or behavior of the weld, it was expected to increase the variability in attenuation found in hole 1, hole 2 from the left, and hole 4 from the right.

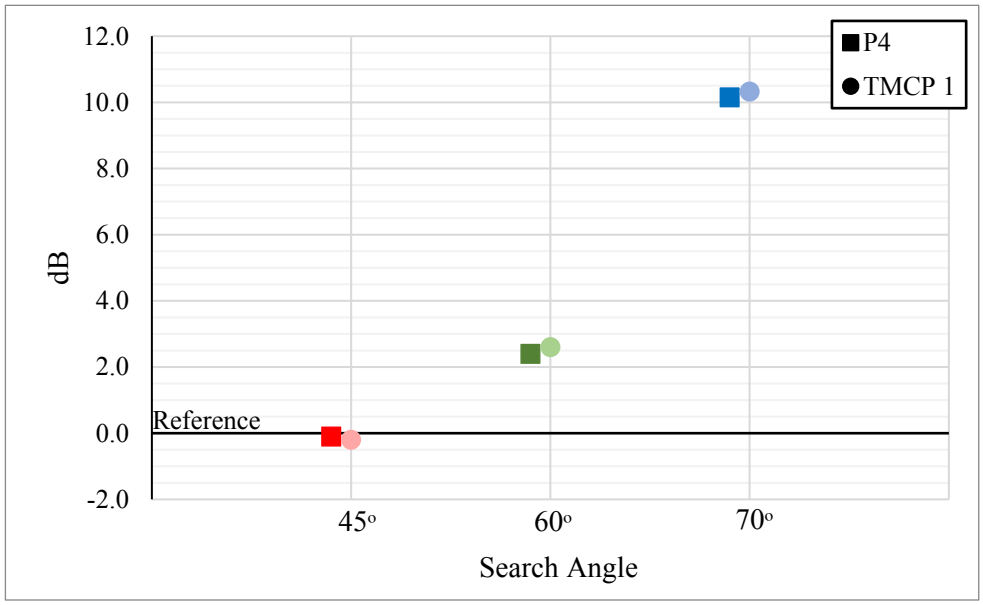

Figure F-38. Specimen P4 versus Specimen TMCP 1 Indication Signal of 0.6" deep hole – 2.25 MHz

Figure F-40 and Figure F-41 show the attenuation per inch of sound path for specimen P4 using a 2.25 MHz and 5 MHz probe, respectively. Again, unlike the trends observed in specimens P1, P2, and P3, the attenuation of hole 1, hole 2 from the left, and hole 4 from the right was inconsistent across different incidence angles and a loss of signal was observed at higher angles. As a result, the attenuation found in hole 2 and hole 4 where the sound path initiated in the weld was more consistent, but still more attenuating than an acoustically isotropic HPS A709 Gr. 70W QT base metal. Similar statements can be said for hole 3 located in the weld metal.

Figure F-42 and Figure F-43 show the overall scatter in attenuation per inch of sound path of all 8 holes located in specimen P4 using 2.25 MHz and 5 MHz probes, respectively. The average attenuation per inch of hole 2 and hole 4 inspected with the sound beam initiating in the weld metal mirrored data collected for specimens P1 and P2 for these holes within ±0.3 dB/in with a 2.25 MHz probe and ±0.5 dB/in with a 5 MHz probe. The average attenuation per inch for hole 3 was similar when compared to specimens P1 and P2 as well with a maximum deviation of ±0.5 dB/in with a 2.25 MHz probe and ±1.3 dB/in deviation with a 5 MHz probe. Overall, when the sound beam initiated and propagated from weld metal and the HAZ less scatter was seen in comparison to the anisotropic base metal.

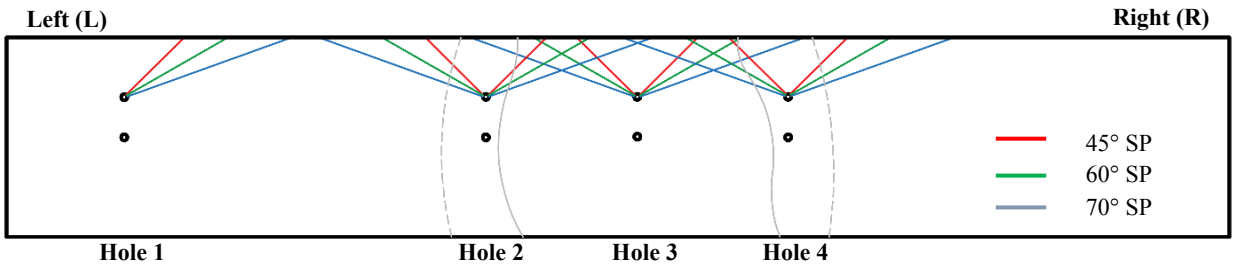

Figure F-39. Specimen P4 Sound Path Schematic – 0.6" deep SDHs

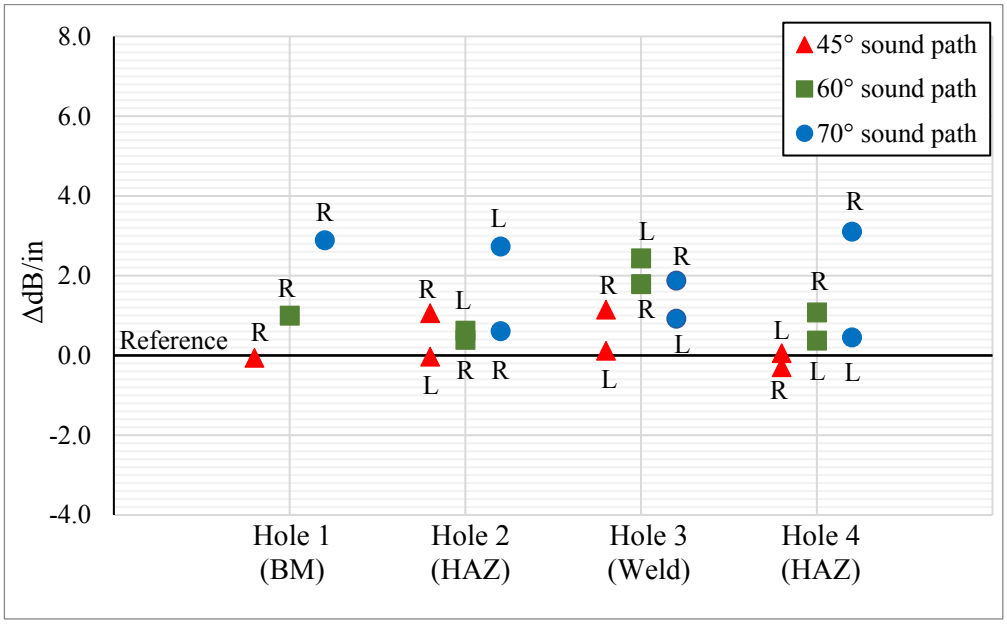

Figure F-40. Specimen P4 Attenuation Per Inch of Sound Path – 0.6 deep hole 2.25 MHz

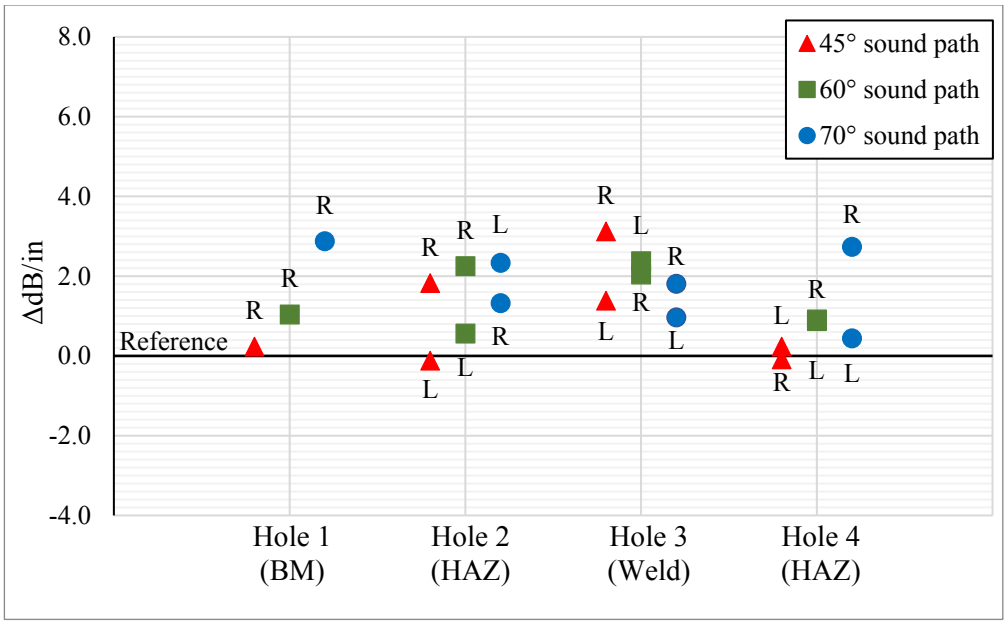

4932
4933 ***Figure F-41. Specimen P4 Attenuation Per Inch of Sound Path– 0.6 deep hole 5 MHz***

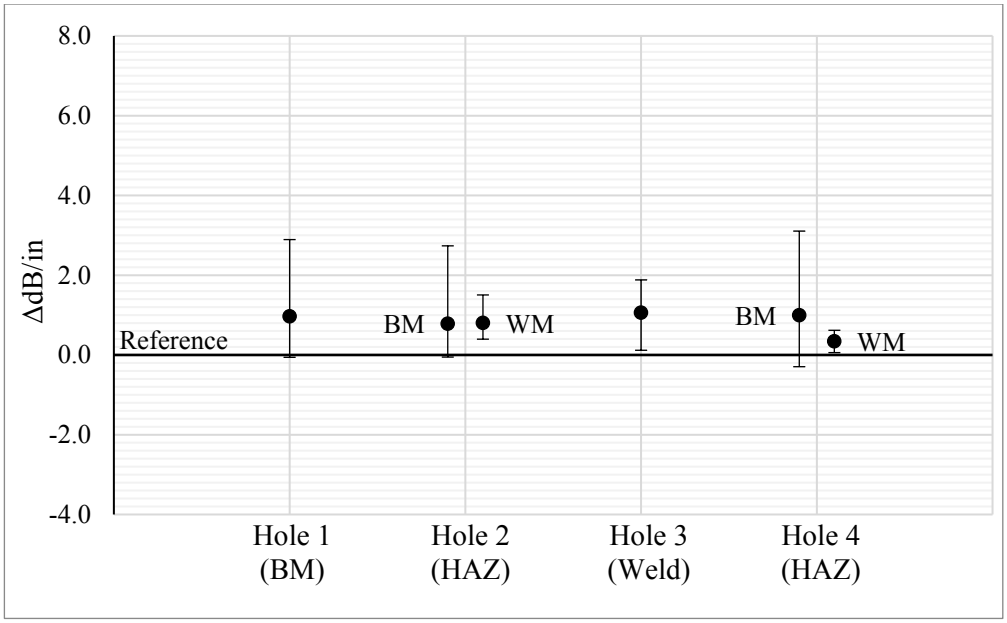

4934
4935 ***Figure F-42. Specimen P4 Attenuation per Inch Overall Scatter –2.25 MHz***

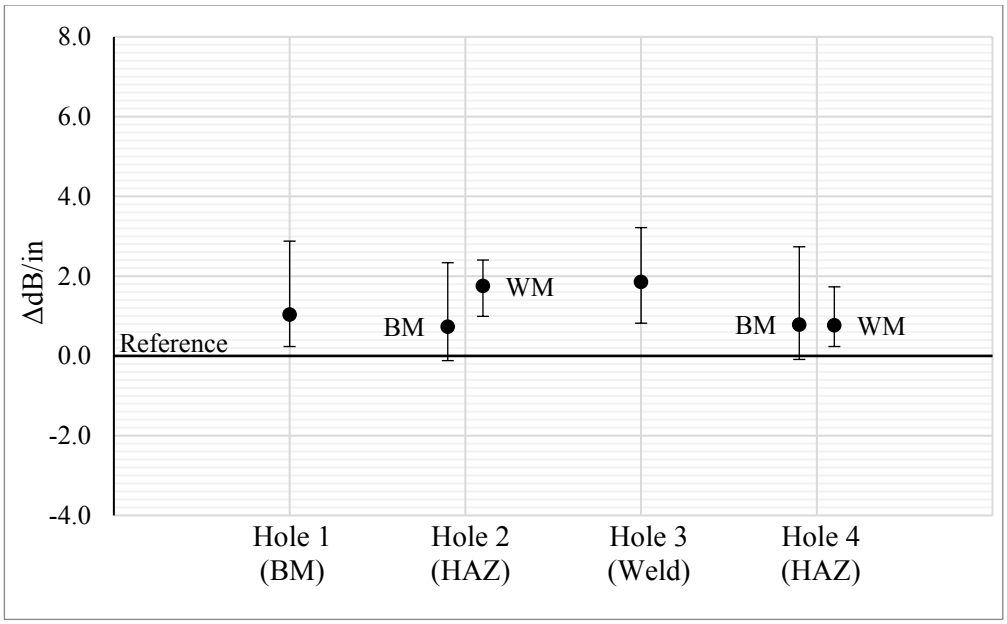

Figure F-43. Specimen P4 Attenuation per Inch Overall Scatter –5 MHz

F.3.5 Conclusions

The ultrasonic inspection of NGI-ESW welds yielded the following conclusions:

- The ultrasonic attenuation of the holes located within the HAZ when shot with sound initiating in the base metal produced very similar results to the holes located solely in base metal. These holes also had very little scatter associated with them, except for Specimen P4 which was acoustically anisotropic.
- The average ultrasonic attenuation and the scatter in results increased when the holes located in the HAZ were shot with the sound initiating in the HAZ or weld metal. The ultrasonic attenuation increased by an average of 0.7 dB/in with a 2.25 MHz probe and 1.3 dB/in with a 5 MHz probe when compared to plain base metal.
- The ultrasonic attenuation was the most inconsistent for the hole located within the weld metal. The ultrasonic attenuation also increased by an average of 1.3 dB/in with a 2.25 MHz probe and 2.3 dB/in with a 5 MHz probe when compared to plain base metal.
- The coarse grain structure of the weld had a clear impact on signal amplitude and attenuation. The inconsistency of results between the two SDHs at the different incidence angle indicated there is a clear variation of the microstructure in the weld, as well.
- The microstructure of the weld impacted the attenuation of sound through NGI-ESW welds too much for probe frequency to make an abundant difference. Therefore, even 2.25 MHz frequency probes still displayed a significant sound loss due to attenuation through the weld metal.

F.4 List of References

[1] K. IBA, "Method of Ultrasonic Angle Beam Examination for Welds of Ferritic Steels with Acoustic Anisotropy," *Trans. Iron Steel Inst. Japan*, vol. 27, no. 11, pp. 898–909, 1987.

[2] N. Rattanasuwannachart, C. Miki, S. Hirose, and H. Shirahata, "Acoustical Anisotropy and Non-Homogeneity of Rolled Steel Plates," *J. Struct. Eng. Eng. Appl. Mech.*, vol. 21, no. 1, p. 1s–9s, 2004.

[3] Japanese Standards Association, *JIS Z 3060:2015 Method for Ultrasonic Testing for Welds of*

Ferritic Steel, 2015th ed. Tokyo, Japan: Japanese Standards Association, 2015.

[4] ASTM, *ASTM E112-13: Standard test methods for determining average grain size*. West Conshohocken, PA: ASTM International, 2013.

[5] E. Papadakis, "Ultrasonic Attenuation and Velocity in SAE 52100 Steel Quenched from Various Temperatures," *Metall. Trans.*, vol. 1, no. April, pp. 1053–1057, 1970.

[6] ISO, *Non-destructive testing - Ultrasonic Testing - Specification for calibration block No. 1 (ISO 2400:2012)*. Brussels: CEN, 2012.

[7] ASME, *ASME BPVC Section V: Nondestructive Examination*, 2017th ed. New York, NY: The American Society of Mechanical Engineers, 2017.

[8] ISO, *ISO 16811:2012 Non-destructive testing - Ultrasonic testing - Sensitivity and range setting*. Brussels: CEN, 2012.

[9] J. J. Chambers and R. D. Medlock, "Electroslag Welding Facts for Structural Engineers," 2015.